Sequential Design of a Linear Quadratic Controller for the Deep Space Network Antennas

W. Gawronski
Ground Antennas and Facilities Engineering Section

A new linear quadratic controller design procedure is proposed for the NASA/JPL Deep Space Network antennas. The antenna model is divided into a tracking subsystem and a flexible subsystem. Controllers for the flexible and tracking parts are designed separately by adjusting the performance index weights. Ad hoc weights are chosen for the tracking part of the controller and the weights of the flexible part are adjusted. Next, the gains of the tracking part are determined, followed by the flexible controller final tune-up. In addition, the controller for the flexible part is designed separately for each mode; thus the design procedure consists of weight adjustment for small-size subsystems. Since the controller gains are obtained by adjusting the performance index weights, determination of the weight effect on system performance is a crucial task. A method of determining this effect that allows an on-line improvement of the tracking performance is presented in this article. The procedure is illustrated with the control system design for the DSS-13 antenna.

I. Introduction

A linear quadratic (LQ) controller design procedure for the Deep Space Network (DSN) antennas is presented. Alvarez and Nickerson [1] have used the LQ approach for controller design of the DSS-14 antenna. In the Alvarez and Nickerson approach, the gearbox flexible mode was included in the rigid-body model of the antenna. In recently designed antenna structures (such as the DSS-13 antenna), significant flexible deformations are observed during tracking operations. The antenna rate-loop model described in [2] consists of 21 flexible modes up to 10 Hz. Controllers for these antennas should suppress flexible motion while following the tracking command. The method presented in this article allows the design of a controller with a flexible motion suppression capability through sequential adjustment of the weights of the LQ performance index.

An LQ controller is optimal in the sense of minimization of the performance index. The tracking performance requirements are reflected in the definition of the performance index through proper adjustment of weights. Indeed, the closed-loop system performance depends heavily on the choice of the weighting matrix, as illustrated with the DSS-13 antenna in Fig. 1. In case 1, the weight 10 for the integral of the antenna position, the weight 1 for the position itself, and the weight 0 for the flexible modes have been chosen. The antenna performance, characterized in this case by its step response in Fig. 1 (solid line), shows excessive flexible motion. In case 2, the weights are the same as those in the previous case, but the weights of the flexible modes are now set equal to 0.001. The closed-loop antenna performance in Fig. 1 (dashed line) shows a significant deterioration of the antenna tracking capabilities.

The procedure presented in [1], as well as other procedures frequently used in antenna design [3], separates controller design for the elevation and azimuth drives. This approach, effective for slow and/or rigid antennas, cannot be justified for fast and/or flexible antennas. In the latter case, the flexible properties of the full antenna significantly differ from the properties of the elevation-only or azimuth-only model of the antenna; thus the separate design of controllers for elevation and azimuth drives would result in system instability. For flexible antennas, there is a quasi-separation of the flexible and tracking motions. This property is used to simplify the controller design procedure. A controller for the flexible part is designed first, followed by a controller for the tracking part, with additional corrections of the controller for the flexible part. The design of the controller for the flexible part is of a sequential nature as well: a controller for each mode is designed separately. The design consists of weight adjustment; it is crucial, therefore, to accurately determine the effect of weight on system performance. The analysis of the impact of weight on system performance is presented in this article. It allows on-line improvement of the tracking performance. The procedure is illustrated with the control system design of the DSS-13 antenna.

II. Properties of a Generic DSN Antenna Model

In this section, study of the properties of an open-loop model (called also a rate-loop model) of a generic Deep Space Network antenna is based on the DSS-13 antenna model. This antenna represents the new generation of 34-meter-diameter antennas. Dynamics of these antennas include non-negligible flexible motion [2], which must be taken into account while designing the tracking controller.

The balanced state-space representation (A_p, B_p, C_p) of the DSS-13 antenna is derived in [2]. Its rate command input is denoted $u_p^T = [u_{pe}\ u_{pa}]$, where u_{pe} and u_{pa} are elevation and azimuth rate commands, respectively, and output is denoted $y_p^T = [y_{pe}\ y_{pa}]$, where y_{pe} and y_{pa} are elevation and azimuth angles. The state vector x_p includes integrator states $x_i^T = [x_{ie}\ x_{ia}]^T$ in elevation and azimuth (rate inputs and position outputs indicate the presence of integrators), and flexible coordinates x_f of dimension n_f; thus,

$$x_p^T = \begin{bmatrix} x_i & x_f^T \end{bmatrix} \tag{1a}$$

The respective state triple is obtained:

$$A_p = \begin{bmatrix} 0 & 0 \\ 0 & A_f \end{bmatrix}, \quad B_p = \begin{bmatrix} B_{pt} \\ B_{pf} \end{bmatrix}, \quad C_p = [C_{pt}\ C_{pf}] \tag{1b}$$

where 0 denotes a zero matrix of proper dimensions.

The matrix C_p, which describes a relationship between the balanced states of the rate-loop model and the elevation and azimuth angles, is small, typically $\|C_p\| < 10^{-3}$ (here and later $\|\cdot\|$ denotes a Euclidean norm). This means that the outputs of the rate-loop system (position angles of the antenna) are much smaller than its states. This property is used later in the controller design procedure.

For controller design purposes, the position angles of the antenna y_p are required to be the first states in the state-space representation. Thus the state x_p is transformed accordingly, so that the new state is

$$x_{pn}^T = [y_p^T\ x_f^T] \tag{2}$$

Since $y_p = C_p x_p$, one obtains the transformation P such that $x_{pn} = P x_p$, where

$$P = \begin{bmatrix} C_p \\ C_r \end{bmatrix} = \begin{bmatrix} C_{pt} & C_{pf} \\ 0 & I_{nf} \end{bmatrix} \tag{3}$$

and $C_r = [0\ I_{nf}]$ (I_{nf} is an identity matrix of dimension n_f). The new state-space representation (A_a, B_a, C_a) is obtained:

$$(A_a, B_a, C_a) = (P A_p P^{-1}, P B_p, C_p P^{-1}) \tag{4}$$

where

$$A_a = \begin{bmatrix} 0 & C_{pf} A_f \\ 0 & A_f \end{bmatrix}, \quad B_a = \begin{bmatrix} B_y \\ B_f \end{bmatrix}$$

$$C_a = [I\ 0], \quad B_y = C_p B_p \tag{5}$$

Additionally, for the controller design purposes, the plant is augmented with the state variables $y_i = [y_{ie},\ y_{ia}]^T$ —an integral of the elevation and azimuth position [1,2]. Thus, by defining the state vector x as

$$x = \left[x_t^T \; x_f^T\right]^T \tag{6}$$

where $x_t = [y_i^T \; y_p^T]^T$, one obtains finally the rate-loop representation (A, B, C):

$$A = \begin{bmatrix} A_t & A_{tf} \\ 0 & A_f \end{bmatrix}, \; B = \begin{bmatrix} B_t \\ B_f \end{bmatrix}, \; C = [C_t \; 0] \tag{7a}$$

where

$$A_t = \begin{bmatrix} 0_2 & I_2 \\ 0_2 & 0_2 \end{bmatrix}, \; A_{tf} = \begin{bmatrix} 0 \\ C_{pf} A_f \end{bmatrix}$$
$$B_t = \begin{bmatrix} 0 \\ C_p B_p \end{bmatrix}, \; C_t = [0_2 \; I_2] \tag{7b}$$

The rate-loop representation in Eq. (7a) is shown in Fig. 2, where the flexible and tracking parts are distinguished. In this representation, B_t is small in comparison with B_f (typically $\|B_t\| / \|B_f\| < 10^{-6}$. Also A_{tf} is small in comparison with A_t and A_f (typically $\|A_{tf}\| < 10^{-3}$, $\|A_f\| > 10$, and $\|A_t\| = 1$). Both properties are the result of a small value of $\|C_p\|$, shown earlier. Thus, the states of the tracking part are much weaker than the states of the flexible part. The strong and weak signal flows are shown in Fig. 2. The strong states of the flexible subsystem and the weak states of the tracking subsystem are shown in Fig. 3, which presents the transfer function plots of the rate-loop systems due to elevation rate command. This property is a foundation of the control design strategy described below.

III. Quasi-Separation of the Flexible and Tracking Subsystems

In the LQ design, the feedback $u = -Kx$ is determined such that the performance index J,

$$J = \int_0^\infty (x^T Q x + u^T R u) \, dt \tag{8}$$

is minimal. The minimum of J is obtained for the gain $K = R^{-1} B^T S$, where S is a solution of the Riccati equation [4]:

$$A^T S + SA - SBR^{-1}B^T S + Q = 0 \tag{9}$$

In the above equations, R is a positive definite input weight matrix, while Q is a positive semidefinite state weight matrix. It is assumed that $R = \rho I$, since both inputs (elevation and azimuth commands) are of equal importance. The further assumption that $\rho = 1$ is made without loss of generality. Divide S and K into parts related to the triple (A, B, C) in Eq. (7a):

$$S = \begin{bmatrix} S_t & S_{tf} \\ S_{tf}^T & S_f \end{bmatrix}, \; K = [K_t \; K_f] \tag{10}$$

so that Eq. (9) can be written as follows:

$$A_t^T S_t + S_t A_t - S_t B_t B_t^T S_t + Q_t - \Delta_{tf} = 0 \tag{11a}$$

$$A_t^T S_{tf} + S_{tf} A_f + S_t A_{tf} - K_t^T K_f = 0 \tag{11b}$$

$$A_f^T S_f + S_f A_f + S_f B_f B_f^T S_f + Q_f - \Delta_{ft} = 0 \tag{11c}$$

where

$$K_t = B_t^T S_t + B_f^T S_{tf}^T \tag{12a}$$

$$K_f = B_t^T S_{tf} + B_f^T S_f \tag{12b}$$

$$\Delta_{tf} = S_t B_t B_f^T S_{tf}^T + S_{tf} B_f K_t \tag{12c}$$

$$\Delta_{ft} = A_{tf}^T S_{tf} + S_{tf}^T A_{tf} - S_{tf}^T B_t K_f + S_f B_f B_t^T S_{tf} \tag{12d}$$

Taking a closer look at Eqs. (12), one can notice that there exist weights Q_t and Q_f such that the gain K_f depends on the flexible subsystem only. Namely, for a large enough matrix Q_f, such that $\|Q_f\| \gg \|\Delta_{ft}\|$, the solution S_f of Eq. (11c) is independent of the tracking subsystem, and for small matrix Q_t one obtains $\|B_t^T S_{tf}\| \ll \|B_f^T S_f\|$. In terms of Eq. (12b), the latter inequality means that the gain K_f depends only on the flexible subsystem. However, due to the weak–strong relationship between flexible and tracking subsystems, the situation is not quite symmetric: There are no Q_t and Q_f such that the gain K_t depends only on the tracking subsystem. To understand this, note that the term small has a different meaning for Q_f and Q_t. Magnitudes of a small matrix Q_f and a small matrix Q_t are of a different order, namely Q_f is small if $\|Q_f\| < 10^{-7}$

and Q_t is small if $\| Q_t \| < 1$. Therefore, increasing Q_t to obtain $\|Q_t\| \gg \|\Delta_{tf}\|$, one obtains $\|B_f^T S_{tf}\|$ and $\|B_t^T S_t\|$ of the same magnitude. According to Eq. (12a), the latter fact means that the gain K_t depends on the flexible subsystem as well as on the tracking subsystem, and the solution S_t of Eq. (11a) is dependent on the flexible subsystem. This property can be validated by observation of the closed-loop transfer functions for different weights as shown in Fig. 4. It follows from the plots that the variations of Q_f changed the properties of the flexible subsystem only, while the variations of Q_t changed the properties of both subsystems.

The independence of the flexible subsystem gains from the tracking subsystem properties is a consequence of small values of B_t, A_{tf}, and Q_t. However, it is required that the weight Q_t be large enough to achieve the required pointing performance. But the increase of Q_t causes the increasing dependency of the flexible subsystem gains on the tracking subsystem. This phenomenon in controller design changes the above independence into a quasi-independence (conditional independence). This property results in a separation of the flexible and tracking parts in the first stage of controller design. Thus the design consists of initial determination of the controller gains of the flexible subsystem followed by adjustment of weights of the tracking subsystem and a final tuning of the flexible weights.

IV. Properties of the LQ Controller for Flexible Structures

The properties of an LQ controller for a flexible subsystem are discussed in this section. In this application, a linear system with distinct complex conjugate pairs of poles and small real parts of the poles is considered a flexible structure. In the following, a balanced state-space representation of a flexible structure is discussed. The balanced representation of flexible structures is close (but not identical) to a modal one [5,6,7]. For LQ synthesis purposes, a balanced rather than modal representation is recommended since the balanced reduction (necessary in controller design) yields more accurate results than the modal reduction, especially for closely spaced poles [8].

Since the LQ controller for the flexible subsystem is determined separately from the tracking subsystem, in this section only the flexible subsystem is considered. Its state-space representation (A, B, C) is controllable and observable (the subscript f is dropped in this section for simplicity of notation), and its controllability (W_c) and observability (W_o) grammians are equal and diagonal, $W_c = W_o = \Gamma$, where Γ is a positive definite diagonal matrix that satisfies the following Lyapunov equations:

$$A\Gamma + \Gamma A^T + BB^T = 0, \quad A^T\Gamma + \Gamma A + C^T C = 0 \quad (13)$$

For a balanced flexible system with n components (or $2n$ states), the balanced grammian has the following form:

$$\Gamma \cong \operatorname{diag}(\gamma_1, \gamma_1, \gamma_2, \gamma_2, \cdots, \gamma_n, \gamma_n) \quad (14)$$

and the matrix A is almost block diagonal [6,7], with dominant 2×2 blocks on the main diagonal:

$$A \cong \operatorname{diag}(A_i), \quad A_i = \begin{bmatrix} -\zeta_i\omega_i & -\omega_i \\ \omega_i & -\zeta_i\omega_i \end{bmatrix}, \; i = 1, \cdots, n \quad (15)$$

where ω_i is the ith natural frequency of the structure and ζ_i is the ith modal damping. The combination of Eqs. (13) and (15) gives

$$\gamma_i(A_i + A_i^T) \cong -B_i B_i^T \cong -C_i^T C_i \quad (16)$$

For the LQ controller defined by Eqs. (8) and (9), it is assumed that

$$Q = \operatorname{diag}(q_i I_2), \text{ and } 0 < q_i \ll 1, \; i = 1, \cdots, n \quad (17)$$

Denote

$$\beta_i = \sqrt{1 + 2q_i\gamma_i/\zeta_i\omega_i} \quad (18)$$

then one obtains Proposition 1.

Proposition 1. $S \cong \operatorname{diag}(s_i I_2)$ is the solution of Eq. (9), where

$$s_i = -0.5\gamma_i^{-1}(1 - \beta_i), \quad i = 1, \cdots, n \quad (19)$$

Proof is presented in the Appendix.

The plots of s_i with respect to $\zeta_i\omega_i$ and γ_i are shown in Fig. 5. They show s_i increases with the weight q_i increase, and s_i decreases with γ_i or $\zeta_i\omega_i$ increase.

Next it will be shown that weighting as in Eq. (17) shifts the ith pair of complex poles of flexible structure, and leaves the remaining pairs of poles almost unchanged. Only the real part of the pair of poles is changed (moving the pole apart from the imaginary axis (see Fig. 6).

Proposition 2. For the weight Q as in Eq. (17) the closed-loop pair of flexible poles $(\lambda_{cri}, \pm j\lambda_{cii})$ is obtained from the open-loop poles $(\lambda_{ori}, \pm j\lambda_{oii})$:

$$(\lambda_{cri}, \pm j\lambda_{cii}) = (\beta_i \lambda_{ori}, \pm j\lambda_{oii}), \quad i = 1, \cdots, n \qquad (20)$$

where β_i is defined in Eq. (18).

For proof see the Appendix.

The real part of the poles is shifted by β_i, while the imaginary part of the poles remains unchanged. The plots of β_i with respect to $\zeta_i\omega_i$ and γ_i are shown in Fig. 7. They show relatively large values of β_i even for small values of q_i, i.e., a significant pole shift to the left. Also, since β_i increases with γ_i and decreases with $\zeta_i\omega_i$, there is a significant pole shift for highly observable and controllable modes with small damping. In terms of the transfer function profile, the weight q_i suppresses the resonant peak at frequency ω_i while leaving the natural frequency unchanged (see Fig. 8 for $i = 1$). Due to weak coupling between modes, the assignment of one mode insignificantly influences other modes. Therefore, the weight assignment is performed either simultaneously for all modes or for each mode separately.

V. Controller Design Algorithm

The LQ controller configuration for the DSN antenna model is shown in Fig. 9(a). The tracking command y_c is compared with the antenna position y_p, and the error $\epsilon = y_p - y_c$ and the integral of the error are the controller inputs.

The procedure for the antenna LQ controller design is sequential. First, for the ad hoc (but relatively small) chosen weights of the tracking subsystem, the weights of the flexible subsystem are determined. Second, the adjustment of the weights of the tracking system is performed, followed by the final adjustment of the weights of the flexible system. The weights of the flexible subsystem are determined sequentially, simplifying the procedure.

The controller order is determined as a part of the weight tuning process. Only the modes that influence the plant performance are considered. If the number of flexible modes is n_f, the number of disregarded modes is n_o, and the size of the tracking system is n_t, then the controller order n_c is

$$n_c = n_t + 2(n_f - n_o) \qquad (21)$$

The following LQ controller design algorithm is proposed:

(1) Determine the plant state-space representation, consisting of flexible and tracking parts, in the form of Eq. (7).

(2) Choose ad hoc but reasonably small weights for the tracking part $Q_t = Q_{\text{tah}}$.

(3) For each balanced coordinate of the flexible part, choose the weight q_i ($i = 1, \cdots, n_f$), and define the weight matrix $Q_{fi} = \text{diag}(0,\ 0,\ \cdots,\ q_i,\ q_i,\ 0,\ 0,\ \cdots,\ 0)$ so that the closed-loop system performance for the weight $Q_i = \text{diag}(Q_{\text{tah}},\ Q_{fi})$ is maximized. For example, determine the weights q_i to impose the required pole shift or to suppress the ith resonant peak to the required level without depreciating other properties of the closed-loop transfer function. Note that for small values of q_i, only the ith pair of poles is shifted (to the left), and the remaining poles are almost unaffected. Disregard the modes for which the weighting does not improve the closed-loop system performance. The resulting weight for the flexible subsystem is

$$Q_f = \sum_{i=1}^{n_f} Q_{fi} \qquad (22)$$

(4) For the already determined weight Q_f, tune weight Q_t to obtain improvements in tracking properties of the antenna.

(5) Adjust the weights of the flexible subsystem, if necessary.

VI. Closed-Loop System

Equations for a closed-loop system with the LQ controller, and with the LQ controller and observer, are derived.

The closed-loop system configuration is shown in Fig. 9(a). The equations for the plant triple (A, B, C), given by Eq. (7) are

$$\dot{x} = Ax + Bu_f, \quad y_p = C_p x, \quad x_f = C_f x \qquad (23)$$

Denoting the output error ϵ and the integral of the error z, one obtains

$$\epsilon = y_p - u = C_p x - u, \quad \dot{z} = \epsilon \qquad (24)$$

thus

$$u_f = k_f C_f x - k_o C_p x - k_i z + k_o u \tag{25}$$

Defining the closed-loop state $x_{cl} = \left[z\ x^T\right]^T$, one obtains the closed-loop equations

$$\dot{x}_{cl} = A_{cl} x_{cl} + B_{cl} u, \quad y_p = C_{cl} x_{cl} \tag{26a}$$

where

$$A_{cl} = \begin{bmatrix} 0 & C_p \\ -Bk_i & A - Bk_f C_f - Bk_o C_p \end{bmatrix}$$

$$B_{cl} = \begin{bmatrix} -I \\ Bk_o \end{bmatrix}, \tag{26b}$$

$$C_{cl} = [0\ C_p]$$

The antenna states are not directly measured; thus the state observer is included in the closed-loop system in Fig. 9(b). Based on plant Eq. (23), the estimator equations are obtained:

$$\dot{\hat{x}} = A\hat{x} + Bu_f + K_e(y_p - \hat{y}_p)$$

$$\hat{y}_p = C_p \hat{x}, \quad \hat{x}_f = C_f \hat{x} \tag{27}$$

The integrator equation

$$\dot{z} = \epsilon = y_p - u = C_p x - u \tag{28}$$

and the nodal equation

$$u_f = -k_f \hat{x}_f - k_o \epsilon - k_i z \tag{29}$$

along with Eqs. (23) and (27) give the equations for the closed-loop system with the state observer

$$\dot{x}_{co} = A_{co} x_{co} + B_{co} u, \quad y = C_{co} x_{co} \tag{30a}$$

where the closed-loop state is $x_{co} = \left[z\ x^T\ \hat{x}^T\right]^T$ and

$$A_{co} = \begin{bmatrix} 0 & C_p & 0 \\ -Bk_i & A - Bk_o C_p & -Bk_f C_f \\ -Bk_i & K_e C_p - Bk_o C_p & A - K_e C_p - Bk_f C_f \end{bmatrix}$$

$$B_{co} = \begin{bmatrix} -1 \\ Bk_o \\ Bk_o \end{bmatrix}, \quad C_{co} = [0\ C_p\ 0] \tag{30b}$$

VII. LQ Controller Design for the DSS-13 Antenna

The DSS-13 antenna model consists of two tracking states (azimuth and elevation angle), and 13 flexible modes (or 26 balanced states). The preliminary weights $q_{ie} = q_{pe} = q_{ia} = q_{pa} = 1$ for the tracking subsystem (for y_i and y_p) and zero weights for the flexible subsystem ($q_1 = q_2 = \cdots = q_{13} = 0$ for all 13 modes) have been chosen for the LQ controller design. The closed-loop system step response is presented in Fig. 10 (elevation and azimuth encoder reading due to elevation and azimuth command) and the magnitudes of the closed-loop transfer function in Fig. 11. Both figures show that flexible motion of the antenna is excessive, and should be damped out. This is achieved by adjusting weights for the flexible subsystem. For the same tracking weights as before, the weight for the first mode (2.32 Hz) is chosen to be $q_1 = 10^{-7}$, and the remaining weights are zero; this obtains the closed-loop system responses shown in Figs. 12 and 13. One can see that the 2.32-Hz resonance peak in the azimuth command response (Fig. 12) has disappeared, as well as most of the flexible motion in the azimuth step response (Fig. 13). The elevation motion is unaffected however, since the azimuth gearbox mode is almost nonexistent in the elevation motion.

The weight should be chosen carefully. Too small a weight (e.g., 3×10^{-9} in the case considered) will not suppress the resonant peak, Fig. 14(a). Too large a weight (e.g., 1×10^{-5}) will deteriorate the tracking performance: For the overweighted mode, the transfer function is pressed down within a wide frequency range, Fig. 14(b). The proper weight suppresses the resonant peak, leaving the other peaks unchanged (Fig. 8).

Next, assuming q_{ie}, q_{ia}, q_{pe}, q_{pa} and q_1 are as given above and setting a weight for the second mode (2.64 Hz) $q_2 = 10^{-7}$ while the remaining weights are zero, one obtains the LQ control system responses shown in Figs. 15 and 16. As a result of a nonzero weight, the 2.64-Hz resonant peak has disappeared in the elevation command motion.

Similar procedures have been applied for the third (4.26-Hz), fourth (3.77-Hz), fifth (7.88-Hz), sixth (4.47-Hz), seventh (3.38-Hz), eighth (5.98-Hz), ninth (7.92-Hz), and tenth (9.48-Hz) modes, with weight 10^{-7} for each mode. As a result, suppression of the remaining flexible motion and resonant peaks is observed in Figs. 17 and 18. Weights for the remaining modes (eleventh through thirteenth) have been set to zero. According to Eq. (21), the controller order is 24 for the plant order of 30.

The root locus of the closed-loop system due to weight variations of the 7.92-Hz mode is shown in Fig. 19. The figure shows the horizontal departure of poles into the left-hand side direction (stabilizing property). It confirms the properties of the weighted LQ design described previously.

In the next step, the tracking properties of the system are improved by proper weight setting of the tracking subsystem. Namely, setting the integral weight to $q_{ie} = q_{ia} = 70$ and the proportional weight to $q_{pe} = q_{pa} = 100$ improves the system tracking properties, as shown in Fig. 20 (small overshoot and settling time) and in Fig. 21 (extended bandwidth—up to 2 Hz). However, by improving the tracking properties, the transfer function has been raised dramatically in the frequency region of 1 to 3 Hz, which forces the first two modes located in this region to appear again in the step response. By sacrificing a bit of the tracking properties, the flexible motion in the step response is reduced. This is done by increasing slightly the weights of the flexible subsystem, setting them as follows: $q_1 = q_2 = q_3 = q_4 = q_5 = q_6 = 10^{-6}$, $q_7 = q_8 = 10^{-7}$, and $q_9 = q_{10} = 10^{-5}$. The closed-loop system response with the satisfactory tracking performance is shown in Figs. 22 and 23 (small overshoot, small settling time, and 1-Hz bandwidth are observed).

VIII. Conclusions

A new procedure for the DSN antenna controller design has been proposed. The antenna model is divided into flexible and tracking parts rather than into elevation and azimuth parts. In a sequential design strategy, a controller for the flexible subsystem is designed first, followed by a controller design for the tracking subsystem. This approach results in a significant improvement of the performance of the antenna closed-loop system through a sequential weight adjustment of the state vector. The properties of the weight adjustment have been quantified in this article. The controller reduction is inherent in this approach. The minimal-order controller is determined through monitoring the closed-loop performance for each flexible mode. The DSS-13 antenna tracking controller design has been used to illustrate the procedure.

Acknowledgment

The author would like to thank B. Parvin for his helpful comments.

References

[1] L. S. Alvarez and J. Nickerson, "Application of Optimal Control Theory to the Design of the NASA/JPL 70-Meter Antenna Axis Servos," *TDA Progress Report 42-97*, vol. January–March 1989, Jet Propulsion Laboratory, Pasadena, California, pp. 112–126, May 15, 1989.

[2] W. Gawronski and J. A. Mellstrom, "Modeling and Simulations of the DSS 13 Antenna Control System," *TDA Progress Report 42-106*, vol. April–June 1991, Jet Propulsion Laboratory, Pasadena, California, pp. 205–248, August 15, 1991.

[3] G. Biernson, *Optimal Radar Tracking Systems*, New York: Wiley-Interscience, 1990.

[4] H. Kwakernaak and R. Sivan, *Linear Optimal Control Systems*, New York: Wiley-Interscience, 1972.

[5] E. A. Jonckheere, "Principal Component Analysis of Flexible Systems—Open Loop Case," *IEEE Trans. on Automat. Control*, vol. AC-29, no. 12, pp. 1095–1097, December 1984.

[6] W. Gawronski and T. Williams, "Model Reduction for Flexible Space Structures," *Journal of Guidance, Control, and Dynamics*, vol. 14, no. 1, pp. 68–76, January 1991.

[7] W. Gawronski and J.-N. Juang, "Model Reduction for Flexible Structures," in *Control and Dynamics Systems*, edited by C. T. Leondes, vol. 36, pp. 143–222, New York: Academic Press, 1990.

[8] T. Williams and W. Gawronski, "Model Reduction for Flexible Spacecraft with Clustered Natural Frequencies," *Proceedings of the 3rd Annual Conference on Aerospace Computational Control*, JPL Publication 89-45, Vol. 2, Jet Propulsion Laboratory, Pasadena, California, p. 620, 1989.

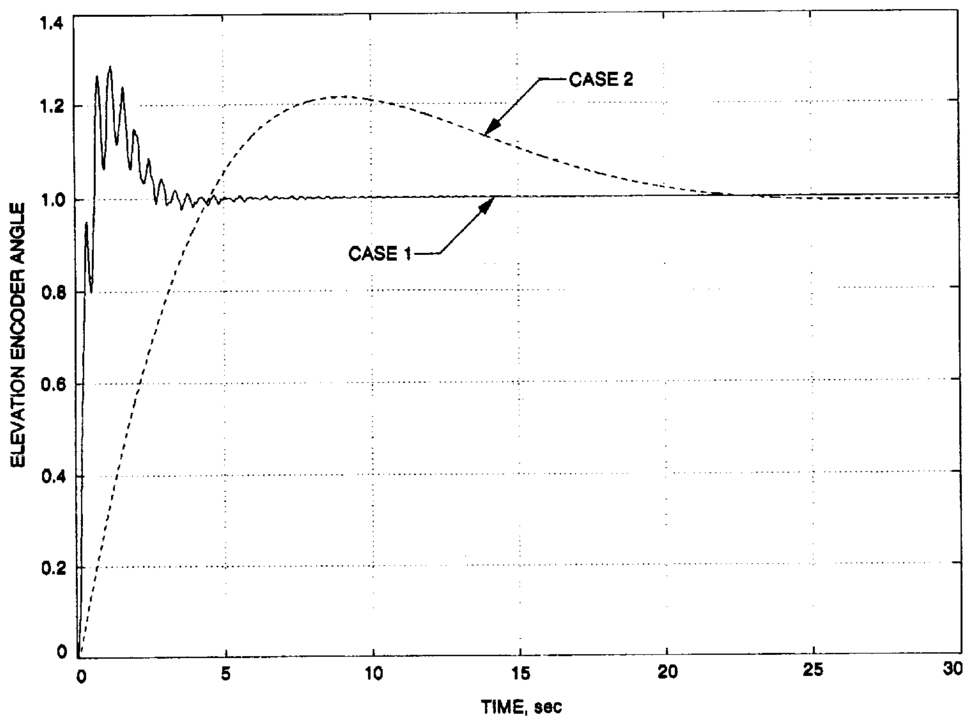

Fig. 1. Step response of the DSS-13 antenna with LQ controller for different weights.

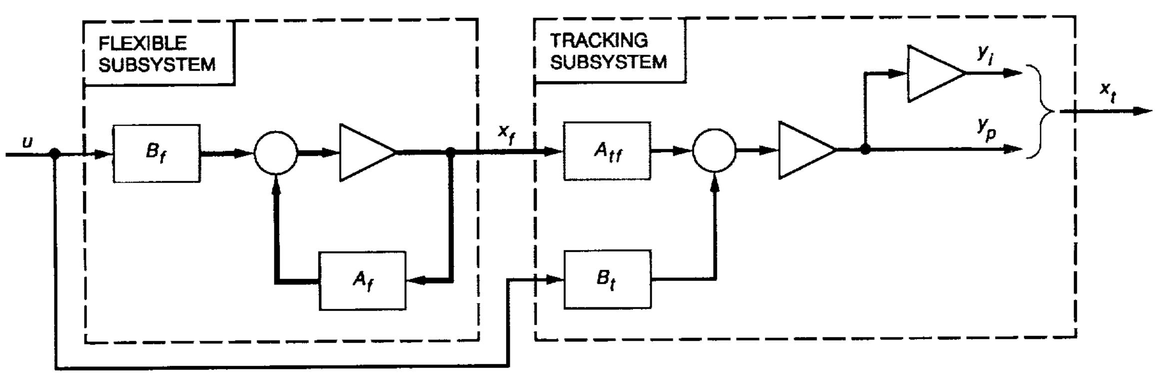

Fig. 2. System configuration.

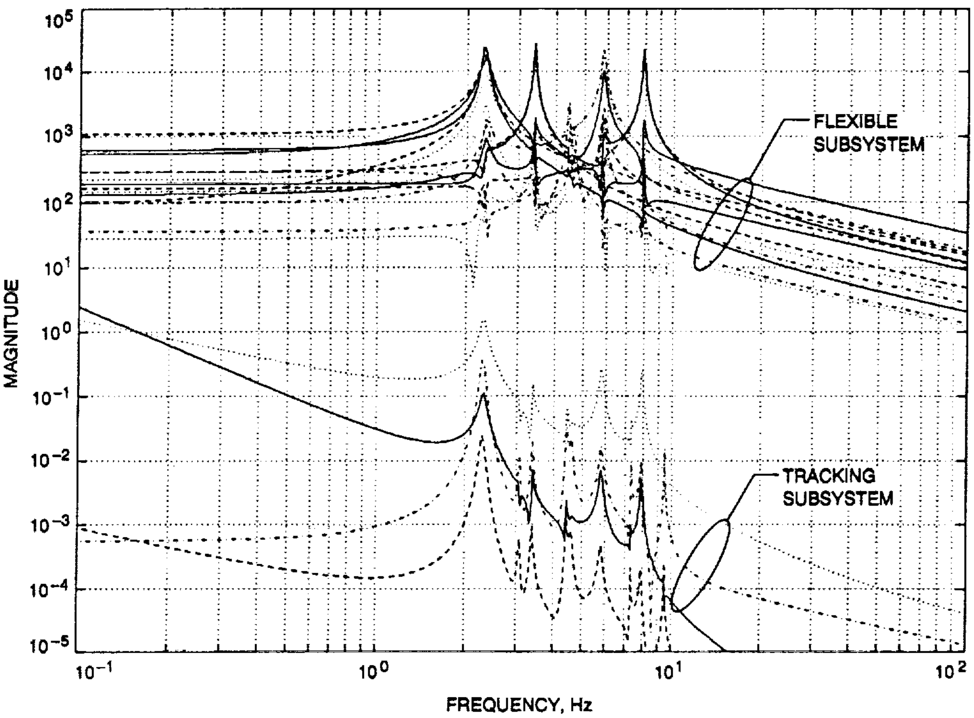

Fig. 3. Magnitude of transfer function of tracking and flexible subsystems for the elevation rate input.

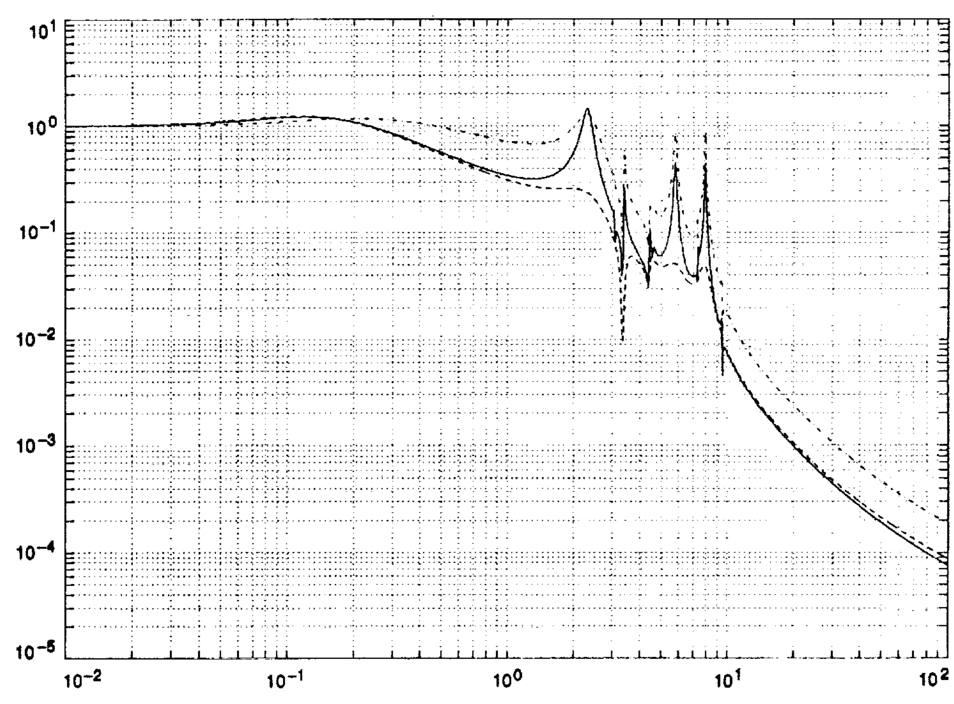

Fig. 4. Magnitude of transfer function of the closed-loop system for different weights: $Q_t = I_4$, $Q_f = 0 \times I_{26}$ (solid line); $Q_t = I_4$, $Q_f = 10^{-7} \times I_{26}$ (dashed line); and $Q_t = 10 \times I_4$, $Q_f = 0 \times I_{26}$ (dot-dashed line).

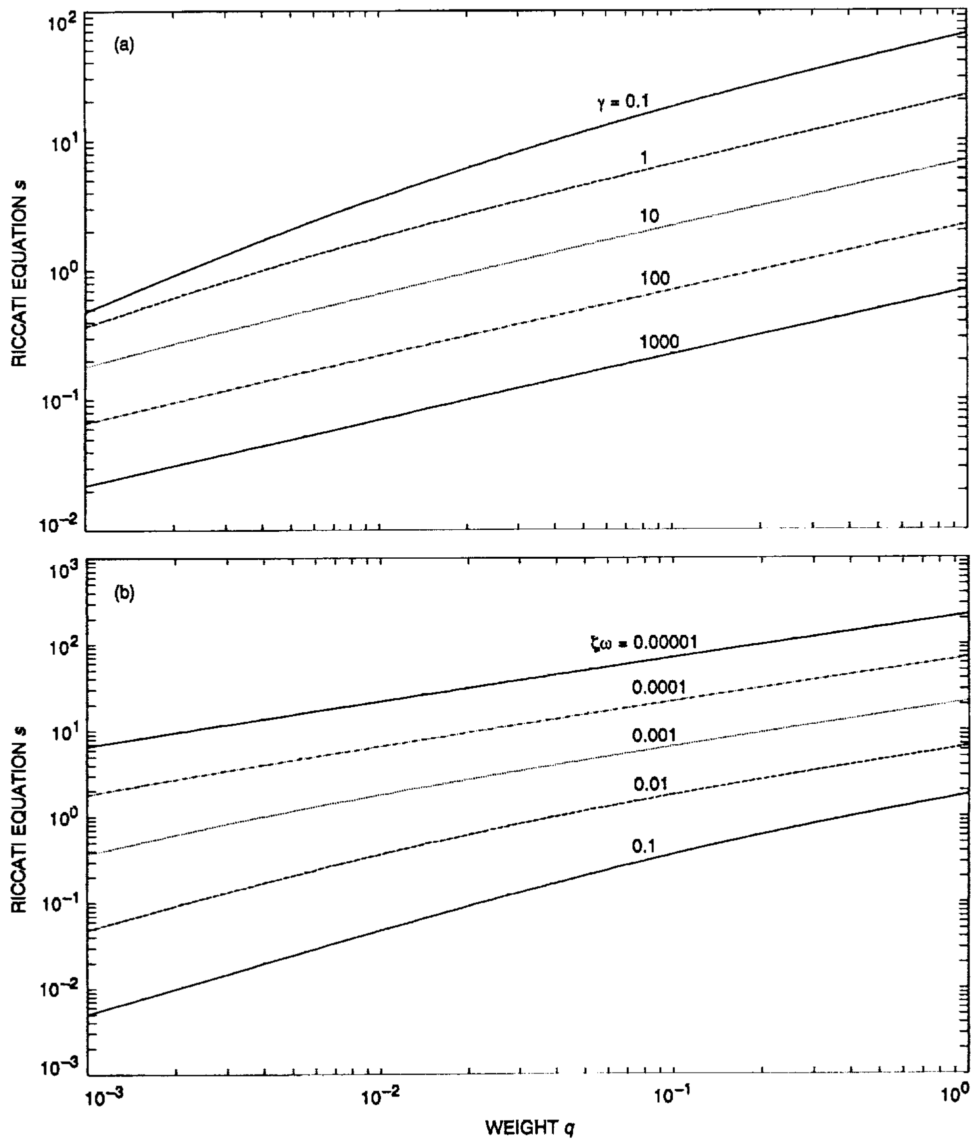

Fig. 5. Solution of the Riccati equation s versus: (a) weight q and Hankel singular value γ and (b) weight q and modal damping $\zeta\omega$.

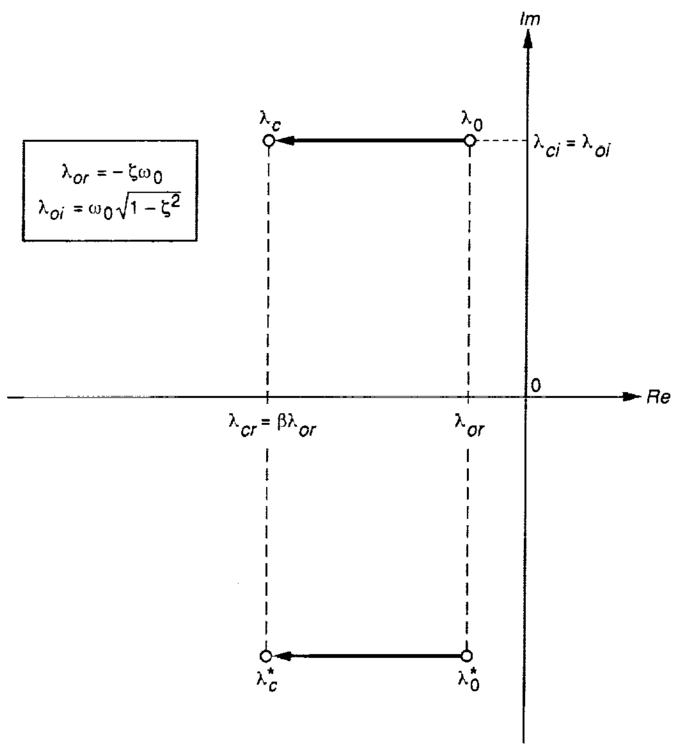

Fig. 6. Location of poles of a flexible structure.

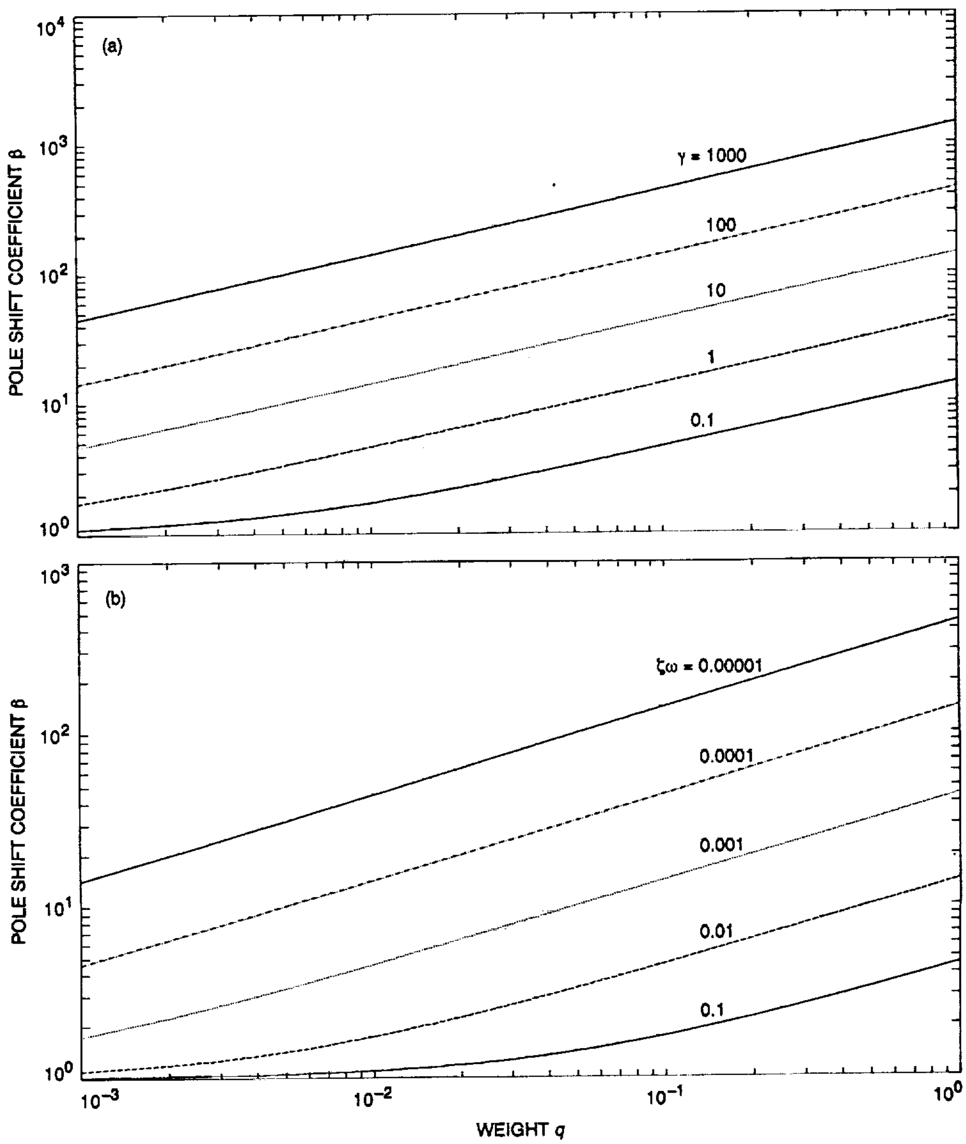

Fig. 7. Pole shift coefficient β versus: (a) weight q and Hankel singular value γ and (b) weight q and modal damping $\zeta\omega$.

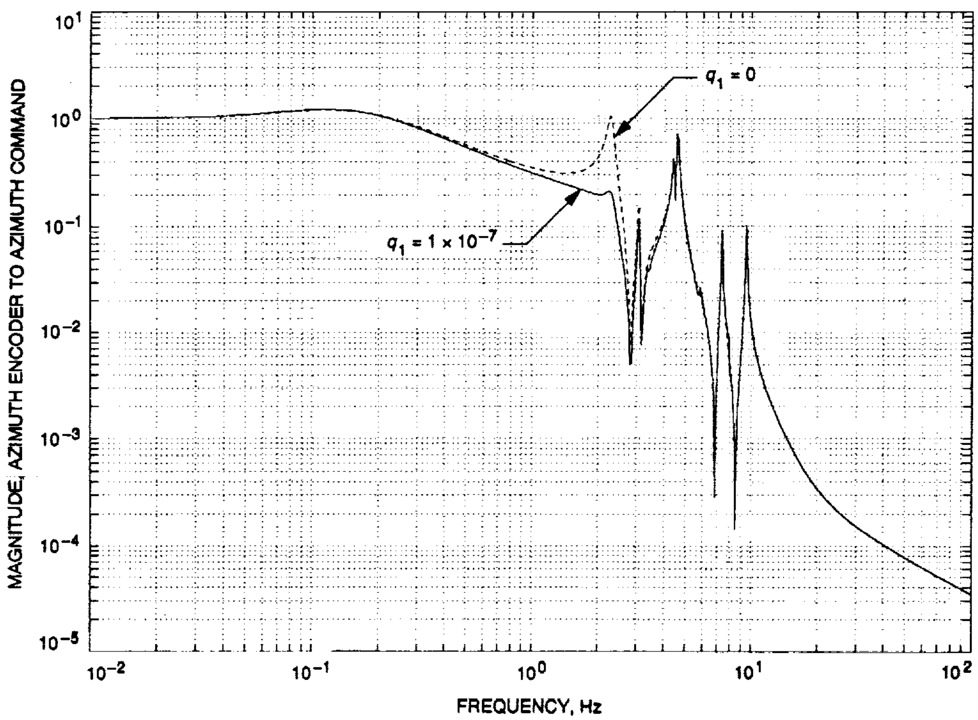

Fig. 8. Vibration suppression with a single weight.

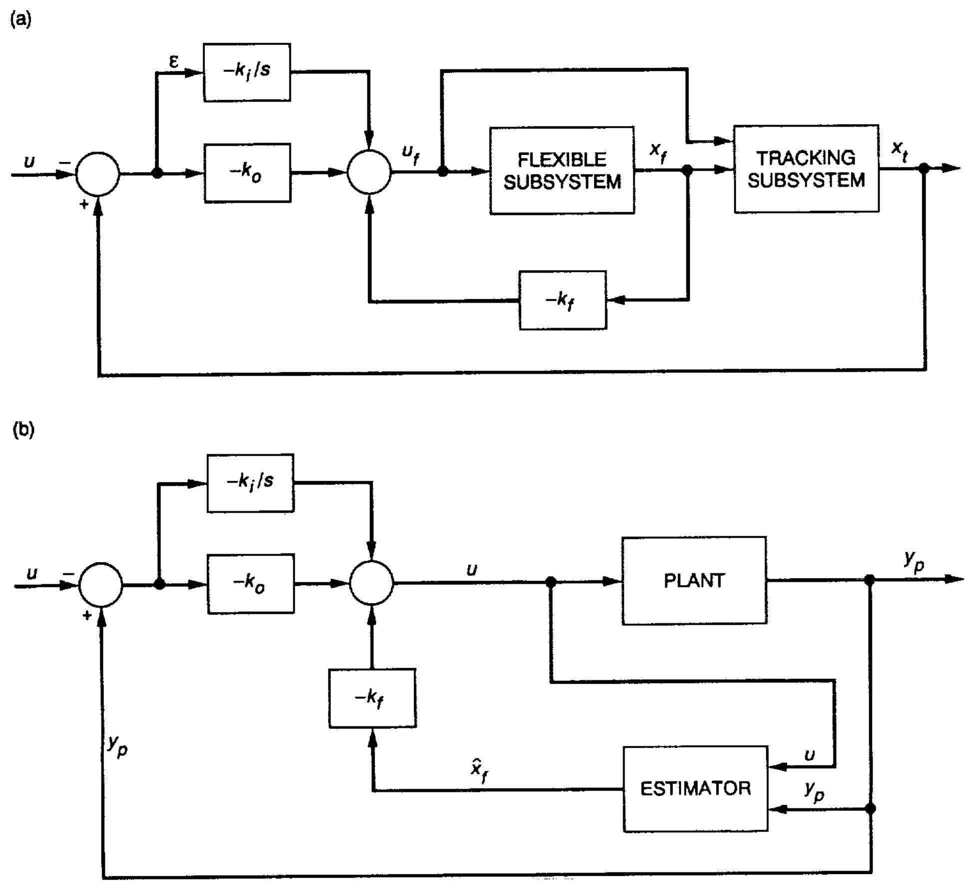

Fig. 9. LQ controller configuration: (a) antenna closed-loop system and (b) antenna closed-loop system with an observer.

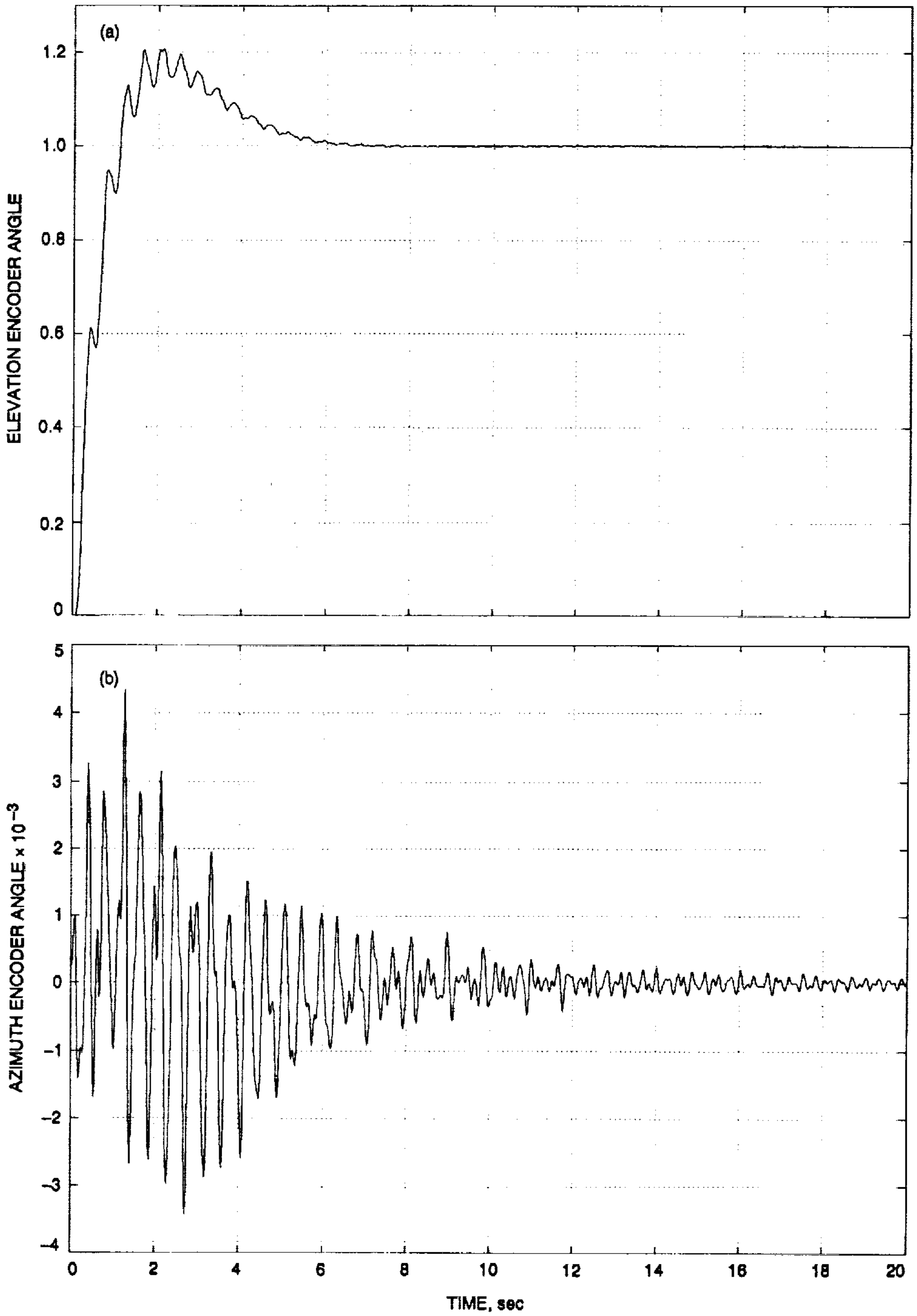

Fig. 10. Closed-loop response to step input for unit proportional and unit integral weights in azimuth and elevation, and zero weight for the flexible subsystem: (a) elevation encoder angle to elevation step command; (b) azimuth encoder angle to elevation step command; (c) azimuth encoder angle to azimuth step command; and (d) elevation encoder angle to azimuth step command.

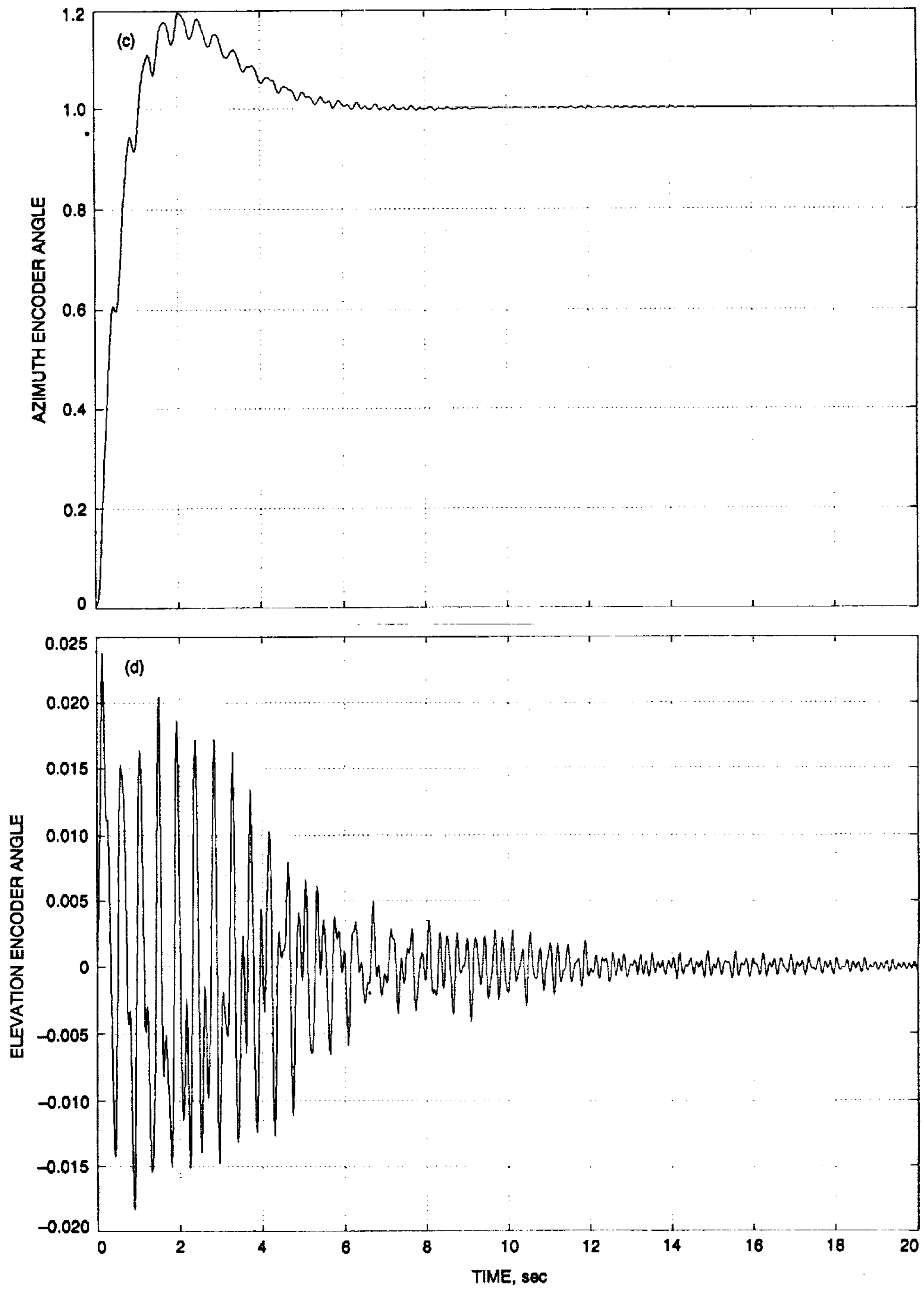
(c)
AZIMUTH ENCODER ANGLE
1.2
1.0
0.8
0.6
0.4
0.2
0
(d)
ELEVATION ENCODER ANGLE
0.025
0.020
0.015
0.010
0.005
0
-0.005
-0.010
-0.015
-0.020
0
2
4
6
8
10
12
14
16
18
20
TIME, sec

Fig. 10 (contd).

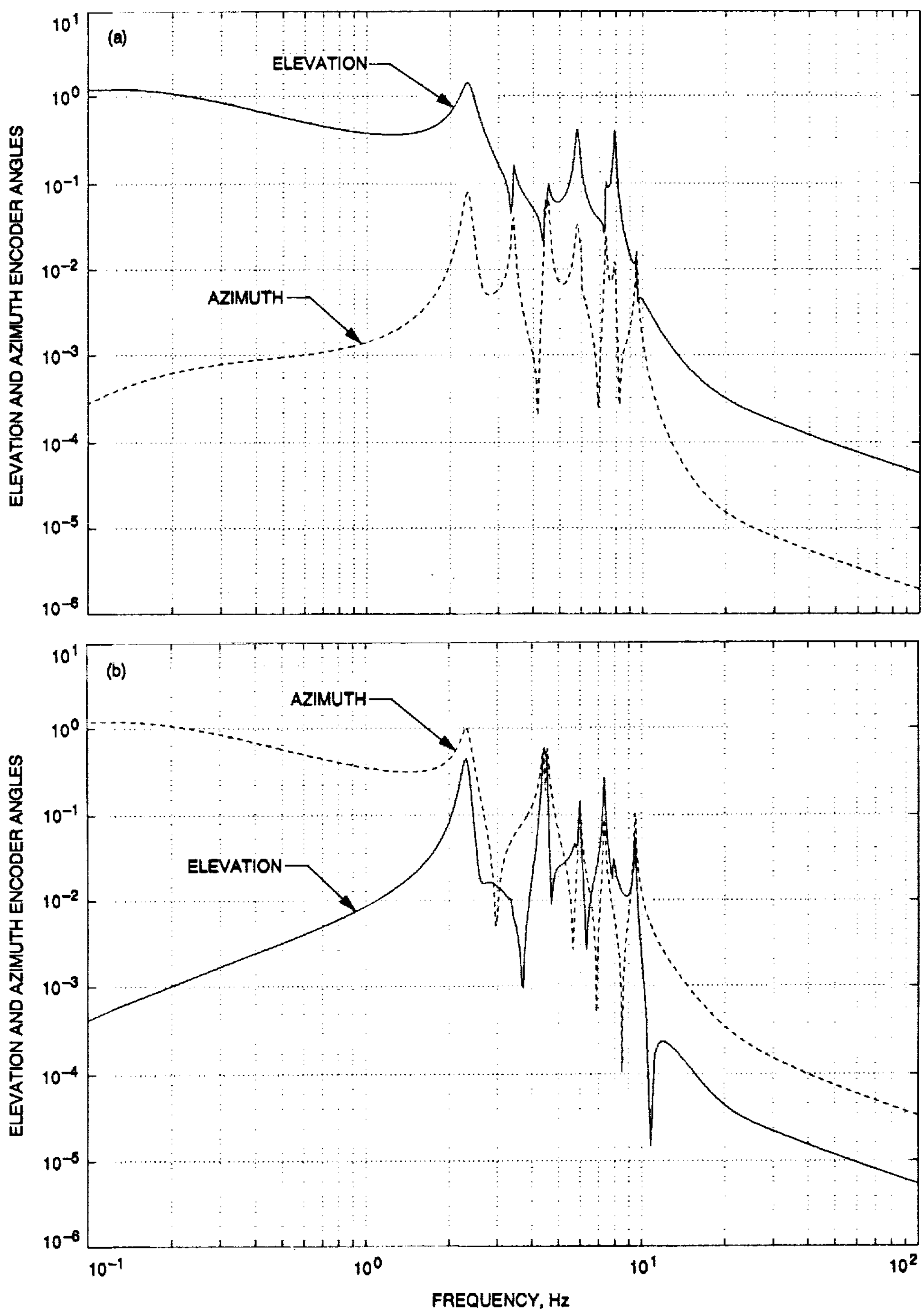

Fig. 11. Closed-loop transfer function for unit proportional and unit integral weights in azimuth and elevation, and zero weight for flexible subsystem: (a) elevation and azimuth encoder angles to elevation step command and (b) elevation and azimuth encoder angles to azimuth step command.

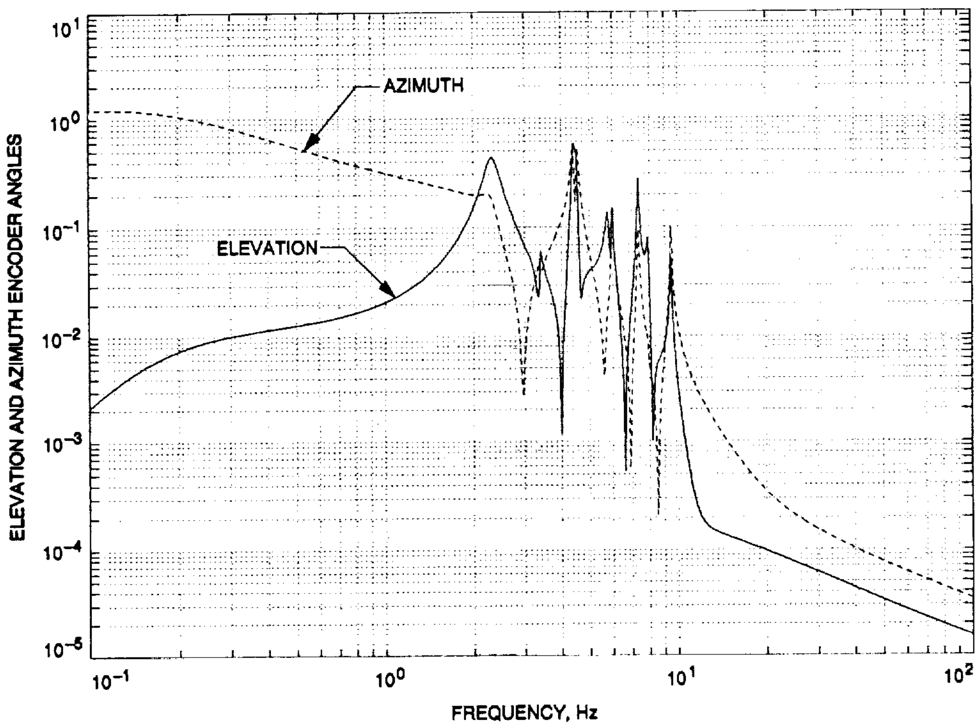

Fig. 12. Transfer function (azimuth and elevation encoder angles to azimuth command) for weights the same as those in Fig. 10, but $q_1 = 1 \times 10^{-7}$.

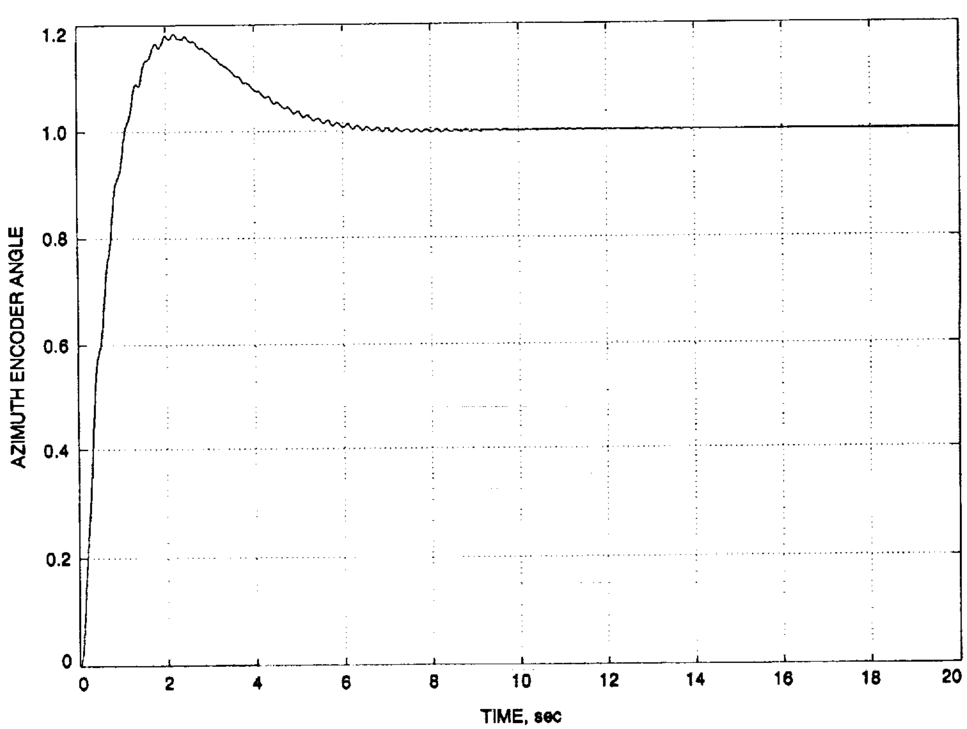

Fig. 13. Azimuth encoder angle step response to azimuth command for weights the same as those in Fig. 12.

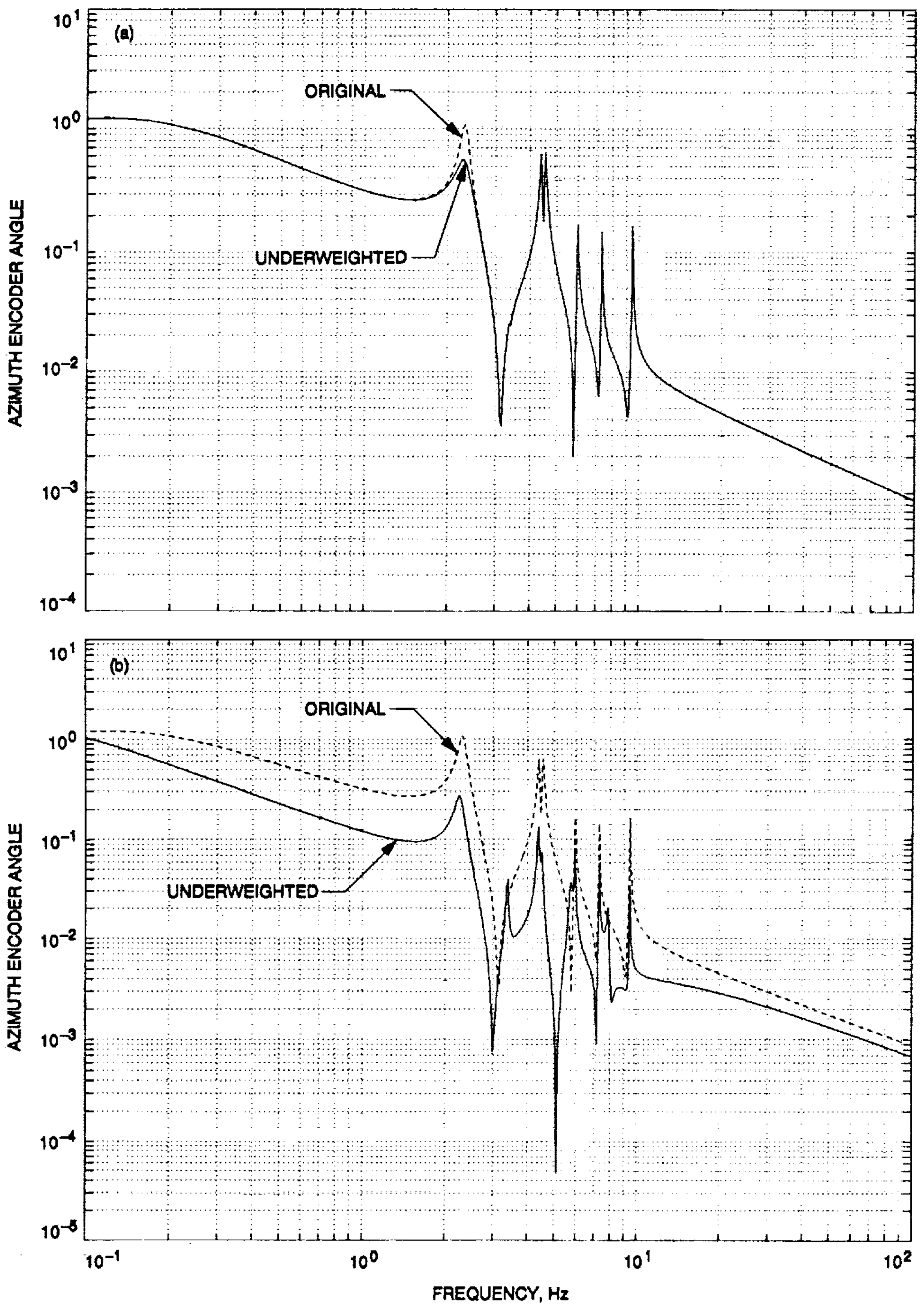

Fig. 14. The first component: (a) underweighted and (b) overweighted.

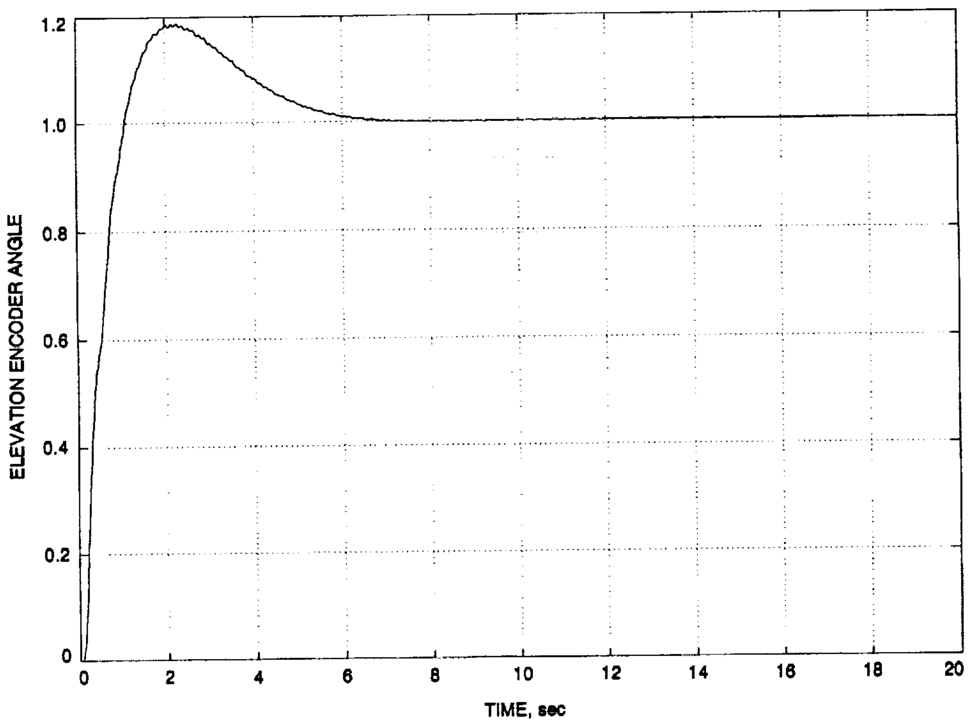

Fig. 15. Elevation encoder angle step response to elevation command for weights the same as those in Fig. 10, but $q_1 = q_2 = 1 \times 10^{-7}$.

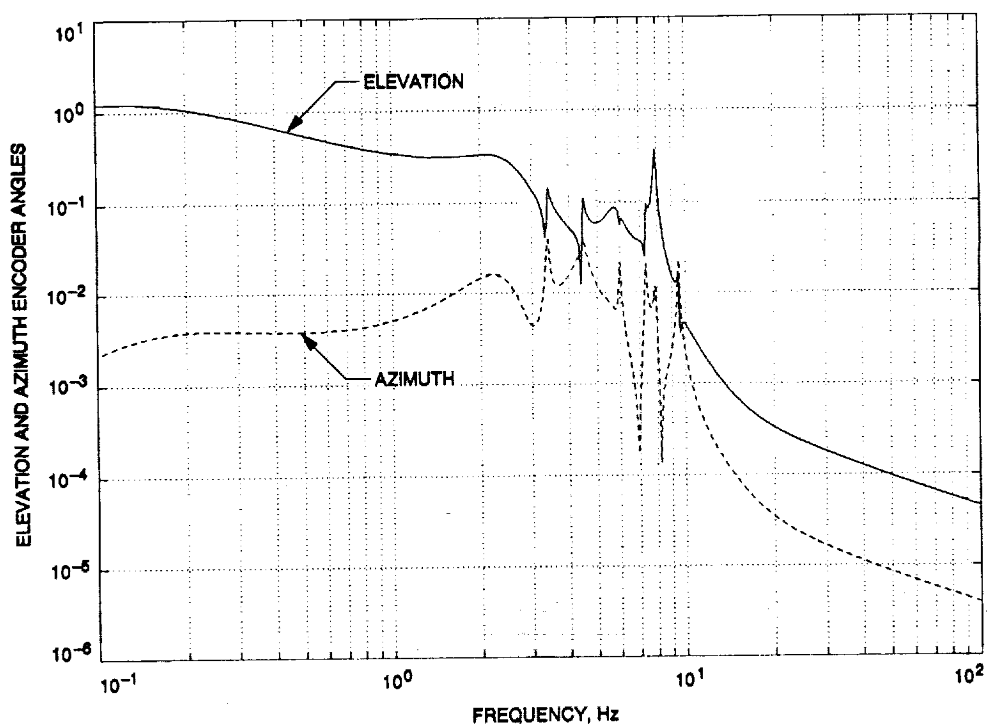

Fig. 16. Transfer function (azimuth and elevation encoder angles to elevation command) for weights the same as those in Fig. 15.

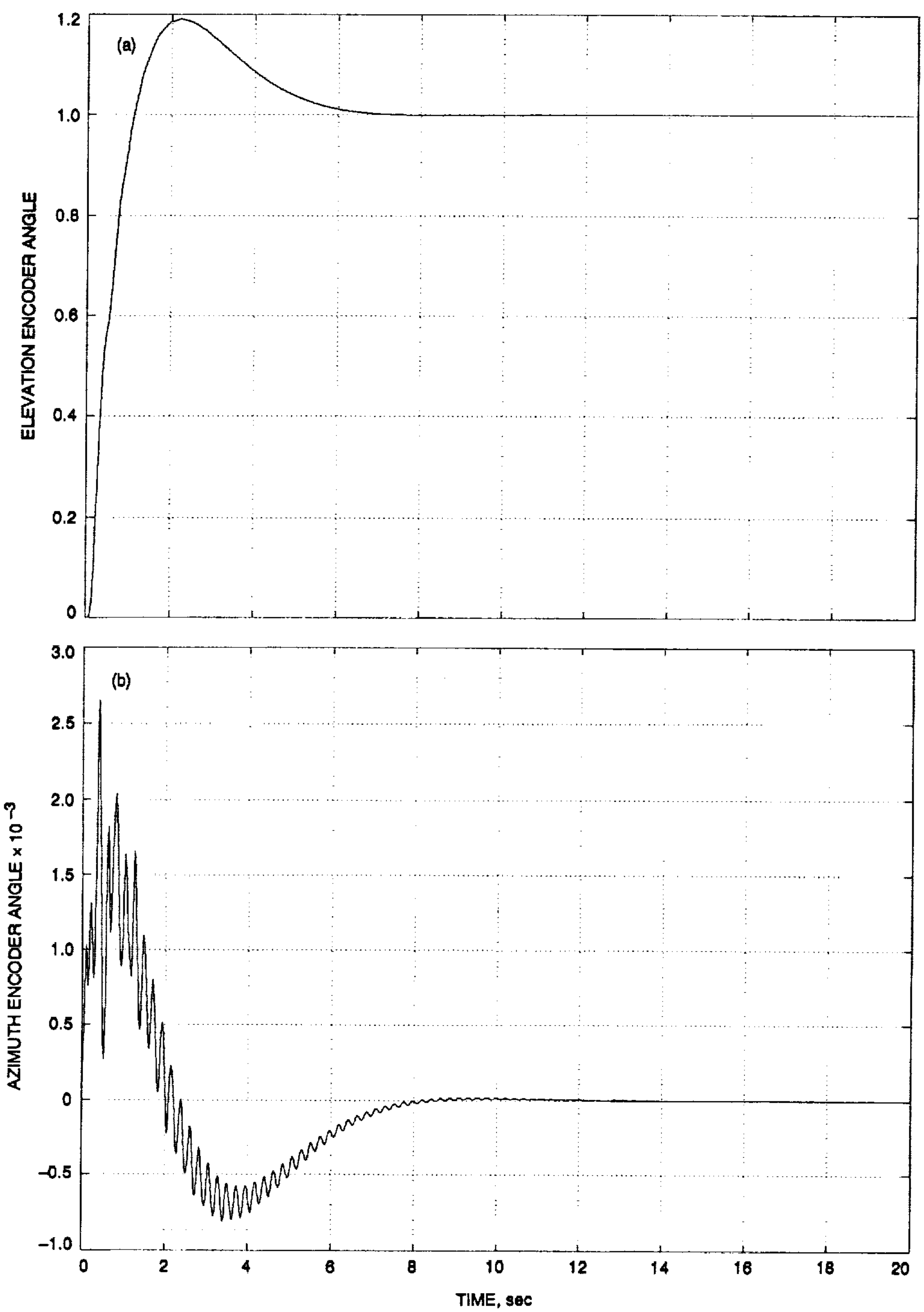

Fig. 17. Closed-loop response to step input for unit proportional and unit integral weights in azimuth and elevation, and weights for the flexible subsystem equal to 1 × 10^{-7}: (a) elevation encoder angle to elevation step command; (b) azimuth encoder angle to elevation step command; (c) azimuth encoder angle to azimuth step command; and (d) elevation encoder angle to azimuth step command.

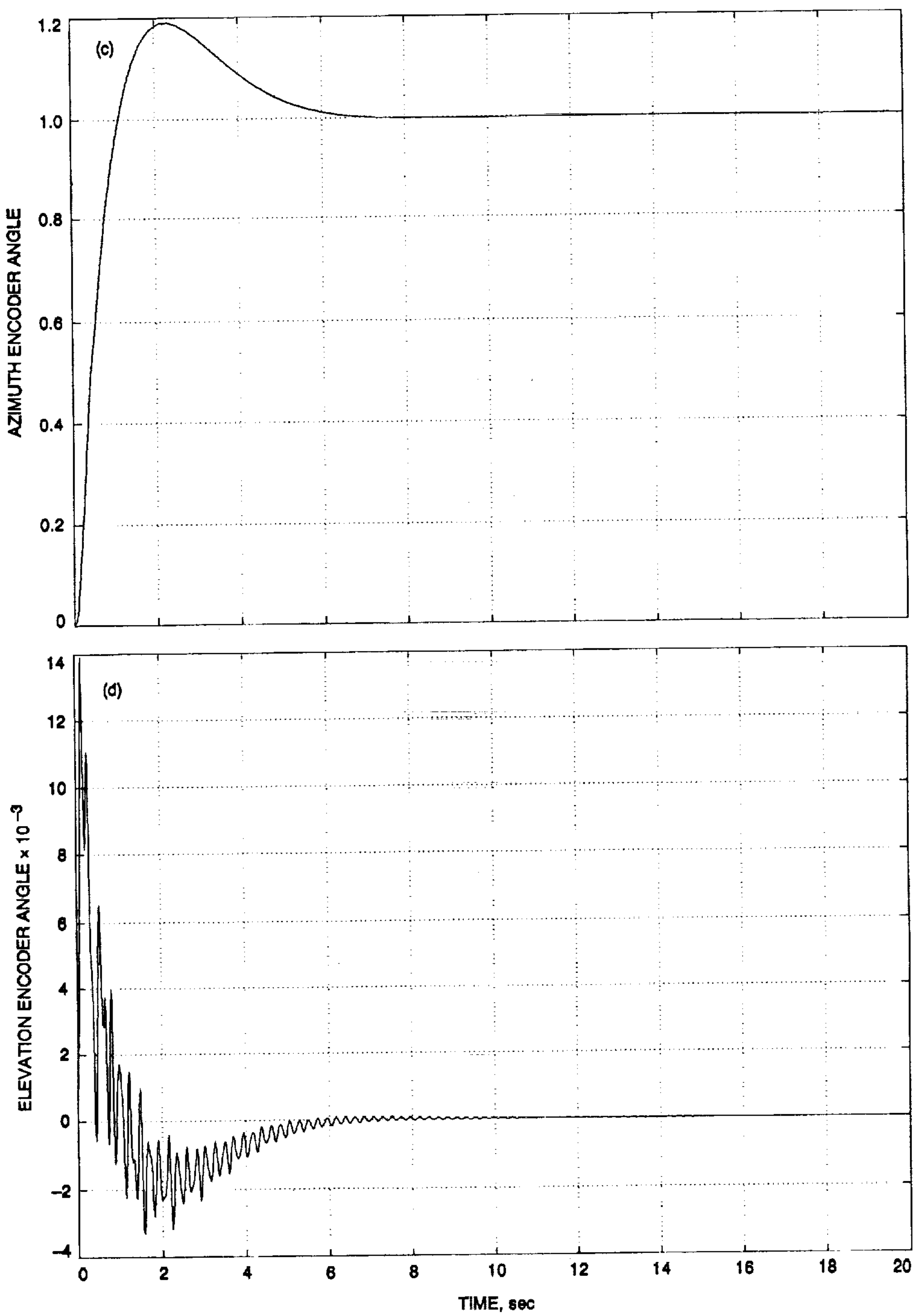

(c)
AZIMUTH ENCODER ANGLE
1.2
1.0
0.8
0.6
0.4
0.2
0
(d)
ELEVATION ENCODER ANGLE × 10 −3
14
12
10
8
6
4
2
0
−2
−4
0
2
4
6
8
10
12
14
16
18
20
TIME, sec

Fig. 17 (contd).

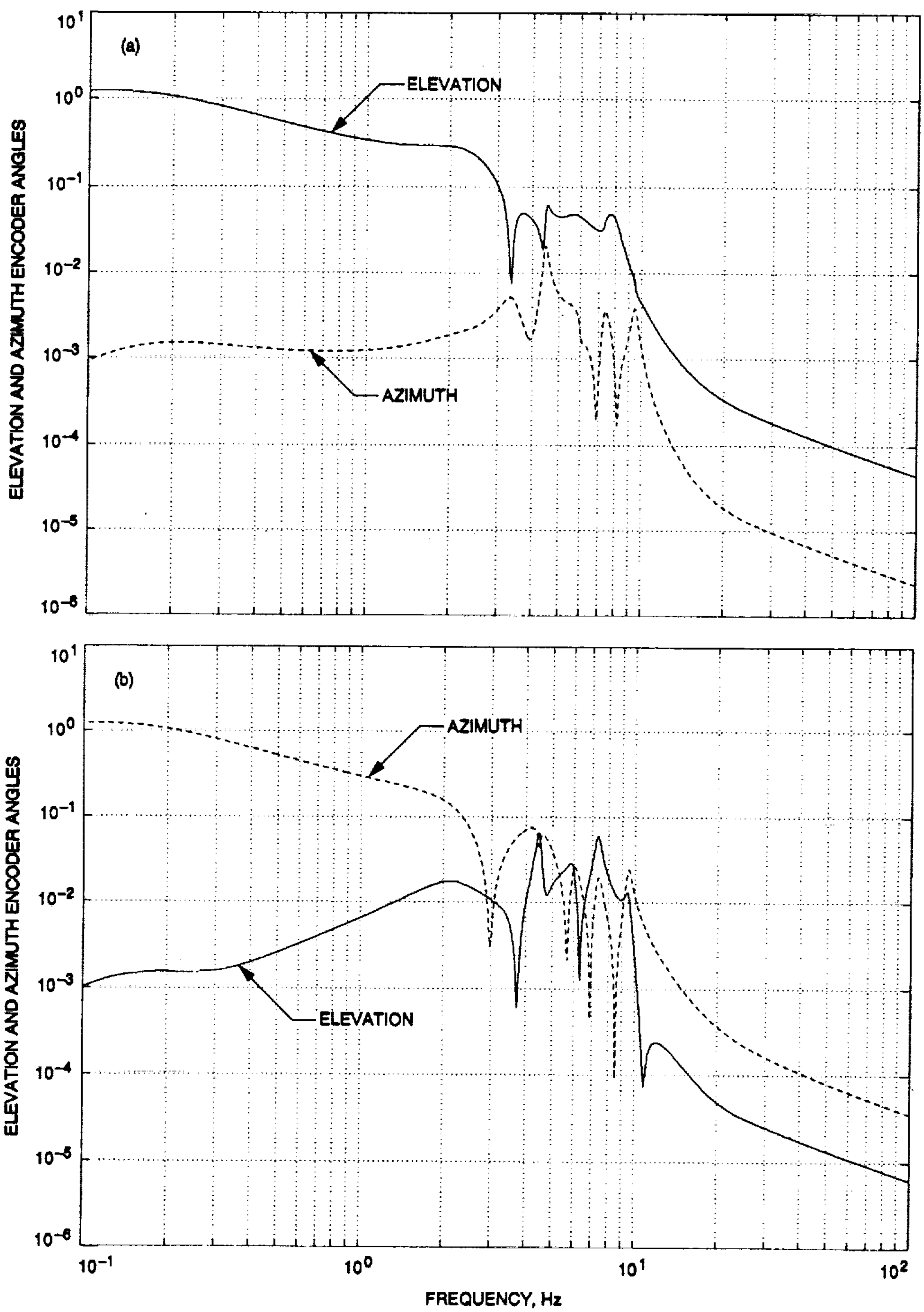

Fig. 18. Closed-loop transfer function for weights the same as those in Fig. 17: (a) elevation and azimuth encoder angles to elevation step command and (b) elevation and azimuth encoder angles to azimuth step command.

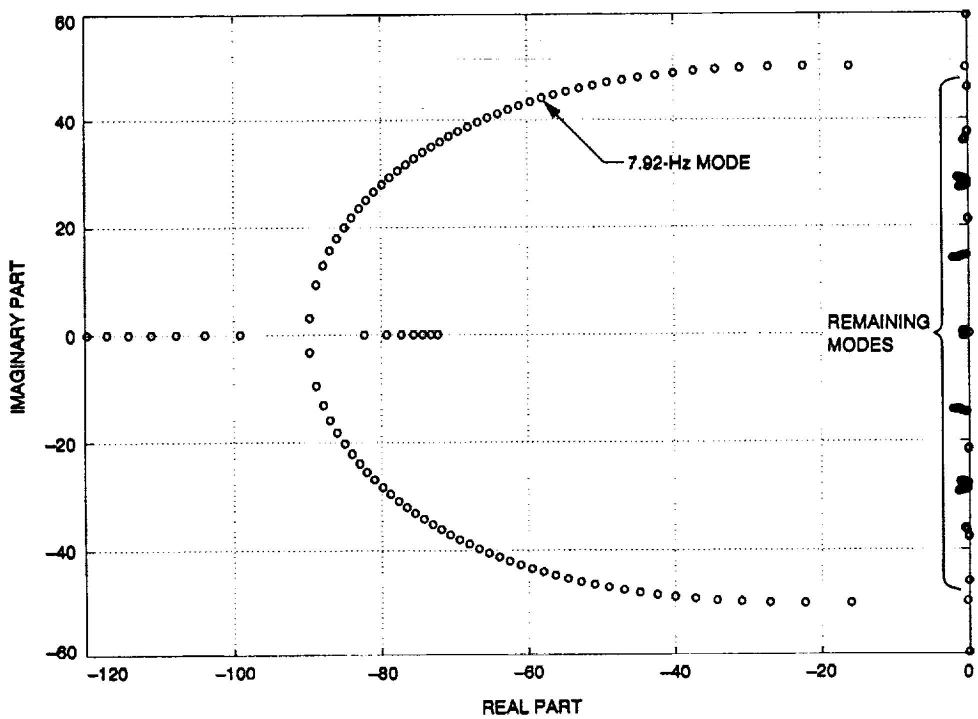

Fig. 19. Root locus for 7.92-Hz mode versus weight.

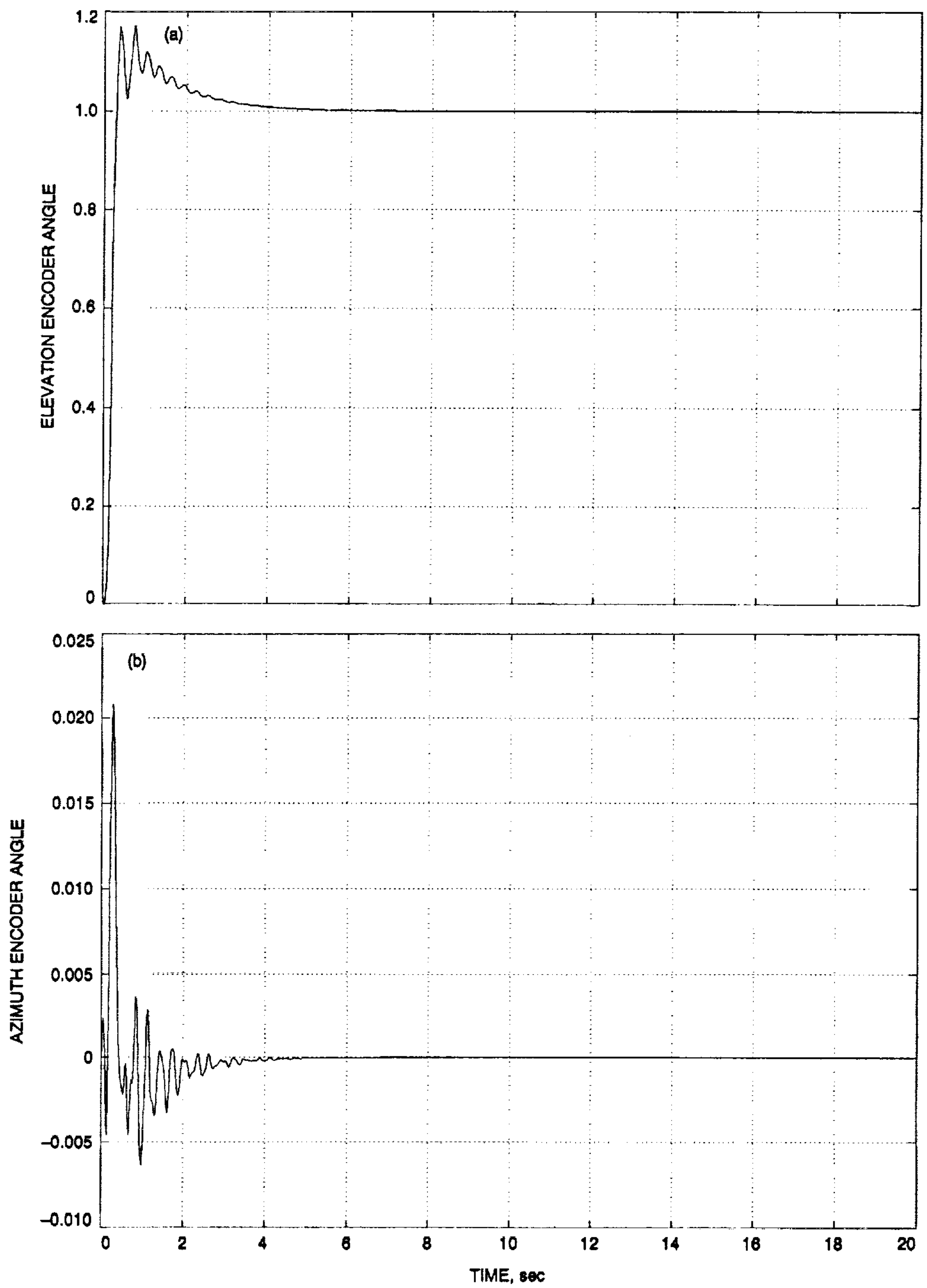

Fig. 20. Closed-loop response to step input for proportional weight 100 and integral weight 70 (both in azimuth and elevation), and weights for the flexible subsystem equal to 1×10^{-7}: (a) elevation encoder angle to elevation step command; (b) azimuth encoder angle to elevation step command; (c) azimuth encoder angle to azimuth step command; and (d) elevation encoder angle to azimuth step command.

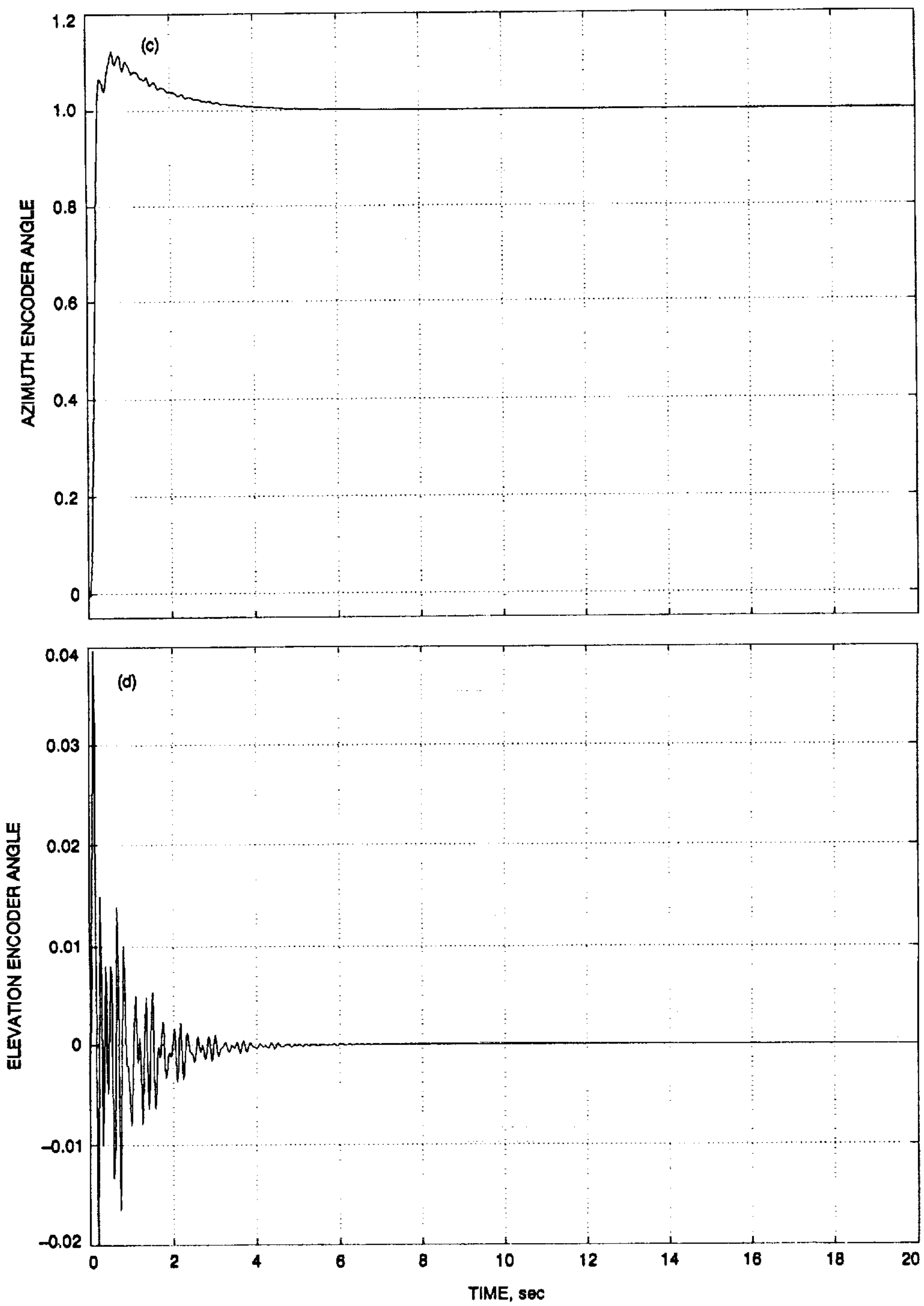
(c)
AZIMUTH ENCODER ANGLE
1.2
1.0
0.8
0.6
0.4
0.2
0
(d)
ELEVATION ENCODER ANGLE
0.04
0.03
0.02
0.01
0
−0.01
−0.02
0
2
4
6
8
10
12
14
16
18
20
TIME, sec

Fig. 20 (contd).

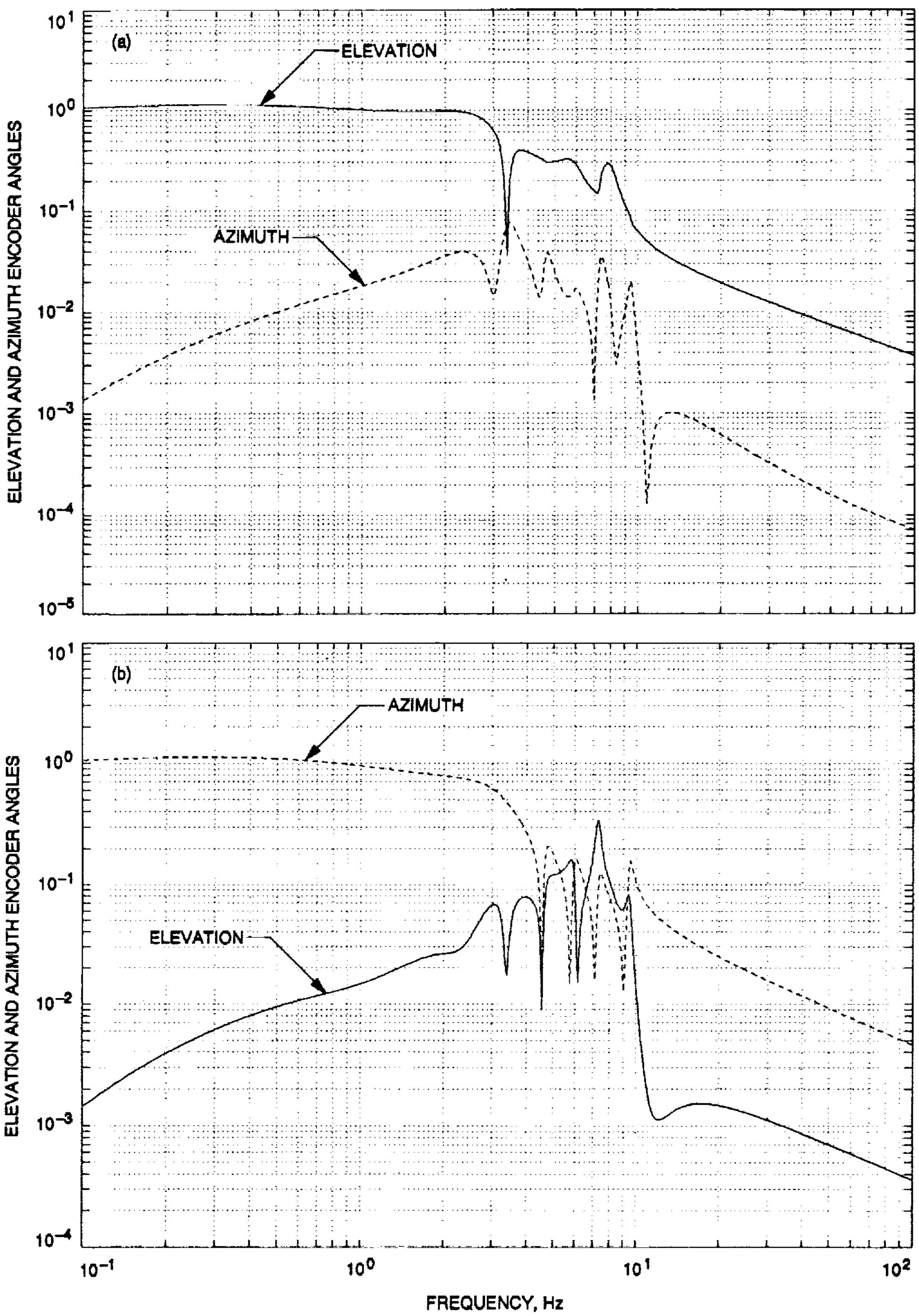

Fig. 21. Closed-loop transfer function for weights the same as those in Fig. 20: (a) elevation and azimuth encoder angles to elevation step command and (b) elevation and azimuth encoder angles to azimuth step command.

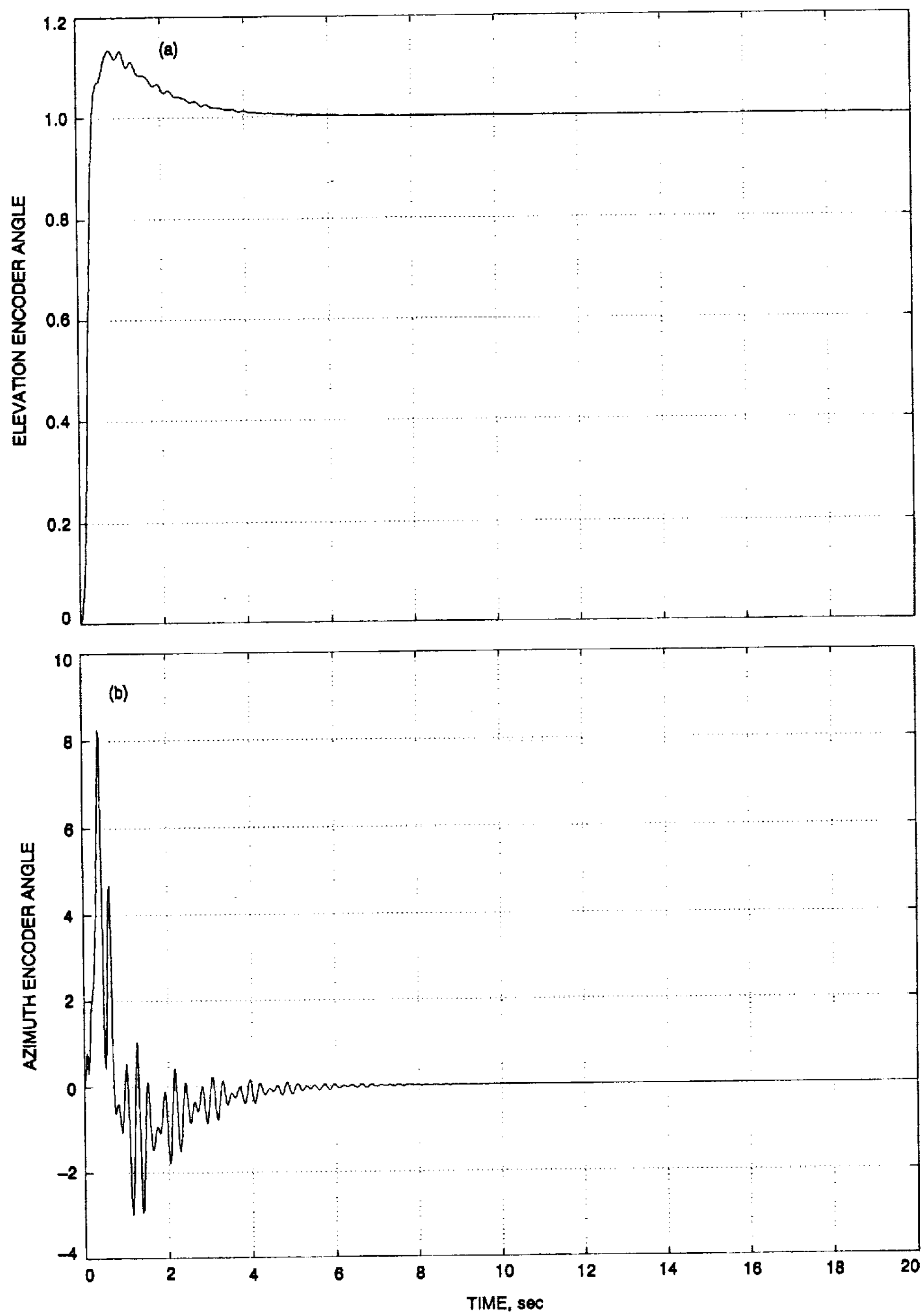

Fig. 22. Closed-loop response to step input for proportional weight 100 and integral weight 70 (both in azimuth and elevation), and weights for flexible subsystem $q_1 = q_2 = q_3 = q_4 = q_5 = q_6 = 1 \times 10^{-6}$, $q_7 = q_8 = 1 \times 10^{-7}$, and $q_9 = q_{10} = 1 \times 10^{-5}$: (a) elevation encoder angle to elevation step command; (b) azimuth encoder angle to elevation step command; (c) azimuth encoder angle to azimuth step command; and (d) elevation encoder angle to azimuth step command.

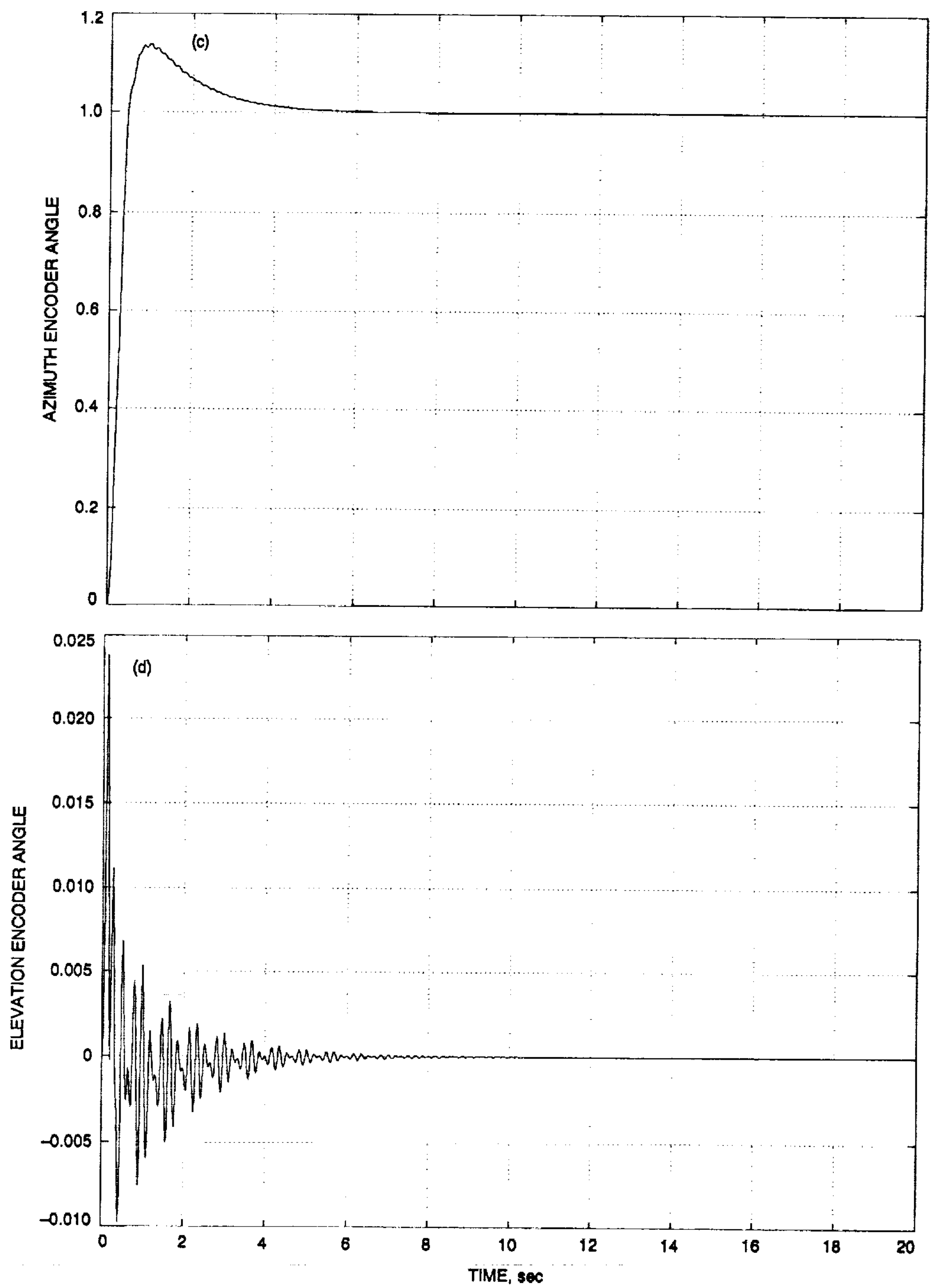
(c)
AZIMUTH ENCODER ANGLE
1.2
1.0
0.8
0.6
0.4
0.2
0
(d)
ELEVATION ENCODER ANGLE
0.025
0.020
0.015
0.010
0.005
0
−0.005
−0.010
0
2
4
6
8
10
12
14
16
18
20
TIME, sec

Fig. 22 (contd).

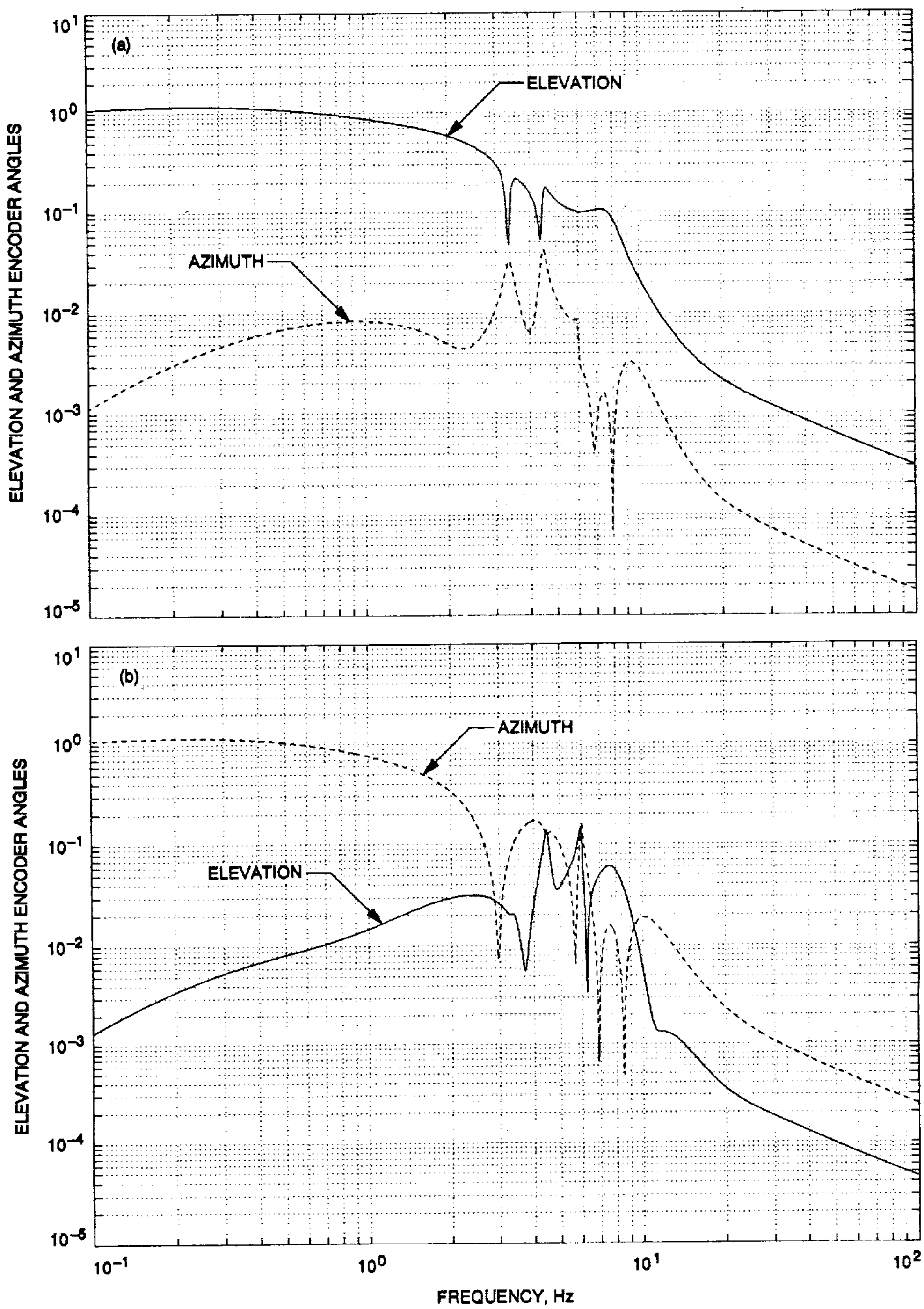

Fig. 23. Closed-loop transfer function for weights the same as those in Fig. 22: (a) elevation and azimuth encoder angles to elevation step command and (b) elevation and azimuth encoder angles to azimuth step command.

Appendix

Proofs

Proof of Proposition 1. For a flexible structure in the balanced representation, the state matrix A is diagonally dominant (with 2×2 blocks on the main diagonal), and for $R = I$ and Q as in Eq. (17), the solution S of the Riccati Eq. (9) is also diagonally dominant with 2×2 blocks S_i on the main diagonal:

$$S_i = s_i I_2, \quad s_i > 0, \quad i = 1, \cdots, n \tag{A-1}$$

Thus, Eq. (9) turns into a set of the following equations:

$$s_i(A_i + A_i^T) - s_i B_i B_i^T + q_i I_2 = 0, \quad i = 1, \cdots, n \tag{A-2}$$

For a balanced system $B_i B_i^T \cong -\gamma_i(A_i + A_i^T)$, see Eq. (16), and for $A_i + A_i^T = -2\zeta_i\omega_i I_2$, see Eq. (15). Therefore, Eq. (A-2) is now

$$s_i^2 + \gamma_i s_i - 0.5 q_i/\zeta_i\omega_i\gamma_i = 0, \quad i = 1, \cdots, n \tag{A-3}$$

There are two solutions of Eq. (A-3), but for $q_i = 0$ it is required that $s_i = 0$. Therefore, Eq. (19) represents the unique solution of Eq. (A-3).

Proof of Proposition 2. For small values of q_i, the matrix A of the closed-loop system is diagonally dominant: $A_o = \mathrm{diag}(A_{oi})$, $i = 1, \cdots, n$, and

$$A_{oi} = A_i - B_i B_i^T s_i \tag{A-4}$$

By introducing Eq. (16) to Eq. (A-4), one obtains

$$A_{oi} = A_i + 2 s_i \gamma_i (A_i + A_i^T) \tag{A-5}$$

and introducing A_i as in Eq. (15) to Eq. (A-5) one obtains

$$A_{oi} = \begin{bmatrix} -\beta_i\zeta_i\omega_i & -\omega_i \\ \omega_i & -\beta_i\zeta_i\omega_i \end{bmatrix} \tag{A-6}$$

with β_i as in Eq. (18).